

DAMPED Ly α SYSTEMS

Arthur M. Wolfe

Department of Physics, and Center for Astrophysics and Space Sciences, University of California, San Diego, Gilman Dr., La Jolla, CA 92093-0424, awolfe@ucsd.edu

Eric Gawiser

NSF Astronomy & Astrophysics Postdoctoral Fellow, Department of Astronomy, Yale University, P.O. Box 208101, New Haven, CT 06520-8108, gawiser@astro.yale.edu

Jason X. Prochaska

University of California Observatories/ Lick Observatory, University of California, 333 Interdisciplinary Science Building, Santa Cruz CA 95064, xavier@ucolick.org

KEYWORDS: cosmology—galaxies: evolution—galaxies: QSOs—absorption lines

ABSTRACT: Observations of damped Ly α systems offer a unique window on the neutral-gas reservoirs that gave rise to galaxies at high redshifts. This review focuses on critical properties such as the H I and metal content of the gas and on independent evidence for star formation. Together, these provide an emerging picture of gravitationally bound objects in which accretion of gas from the IGM replenishes gas consumed by star formation. Other properties such as dust content, molecular content, ionized-gas content, gas kinematics, and galaxy identifications are also reviewed. These properties point to a multi-phase ISM in which radiative and hydrodynamic feedback processes are present. Numerical simulations and other types of models used to describe damped Ly α systems within the context of galaxy formation are also discussed.

CONTENTS

WHAT ARE THE DAMPED Ly α SYSTEMS and HOW ARE THEY FOUND? . . .	2
<i>History of damped Lyα Surveys</i>	3
<i>Modern Surveys and Identification of damped Lyα systems</i>	5
<i>The Significance of the $N(\text{H I}) \geq 2 \times 10^{20} \text{ cm}^{-2}$ Survey Threshold</i>	7
THE NEUTRAL GAS CONTENT OF THE UNIVERSE	7
<i>Formalism</i>	7
<i>$f(N, X)$</i>	8
<i>dN/dX</i>	9
<i>$\Omega_g(z)$</i>	9
<i>Model Comparisons</i>	11
CHEMICAL ABUNDANCES	13
<i>Methodology</i>	13
<i>Metallicity</i>	15
<i>Relative Abundances</i>	17

IONIZED GAS	20
MOLECULAR GAS	21
KINEMATICS	23
GALAXY IDENTIFICATIONS	25
<i>Galaxies with $z \geq 1.6$</i>	25
<i>Galaxies with $z < 1.6$</i>	27
STAR FORMATION IN DAMPED $\text{Ly}\alpha$ SYSTEMS	28
<i>Direct Emission Measurements of Star Formation Rates in Damped $\text{Ly}\alpha$ Systems with $z > 1.6$</i>	28
<i>Star Formation Rates from the C II* Technique</i>	29
<i>Implications</i>	31
CHEMICAL EVOLUTION MODELS for DAMPED $\text{Ly}\alpha$ SYSTEMS	32
ARE DAMPED $\text{Ly}\alpha$ SAMPLES BIASED BY DUST?	34
<i>Observational estimates of reddening</i>	34
<i>Surveys of radio-selected QSOs</i>	35
<i>Empirical Estimates of Damped $\text{Ly}\alpha$ System Obscuration</i>	35
ARE DAMPED $\text{Ly}\alpha$ SAMPLES BIASED BY GRAVITATIONAL LENSING ?	36
CONCLUSIONS	36

1 WHAT ARE THE DAMPED $\text{Ly}\alpha$ SYSTEMS and HOW ARE THEY FOUND?

Damped $\text{Ly}\alpha$ systems are a class of QSO absorbers selected for the presence of H I column densities, $N(\text{H I}) \geq 2 \times 10^{20} \text{ cm}^{-2}$. This criterion differs from those used to find other classes of QSO absorbers selected on the basis of H I content. The $\text{Ly}\alpha$ forest absorbers, reviewed in this journal by Rauch (1998), are selected for $N(\text{H I}) < 10^{17} \text{ cm}^{-2}$, while the Lyman limit systems have $10^{17} < N(\text{H I}) < 2 \times 10^{20} \text{ cm}^{-2}$ (Peroux et al. 2003b). The $\text{Ly}\alpha$ forest absorbers are optically thin at the Lyman limit, since the column density $N(\text{H I}) = 10^{17} \text{ cm}^{-2}$ corresponds to about unity optical depth at the Lyman limit. Are these absorbers physically different from the damped systems or have the column-density criteria resulted in arbitrary distinctions? In fact there is a fundamental difference: hydrogen is mainly neutral in damped $\text{Ly}\alpha$ systems, while it is ionized in all other classes of QSO absorption systems. This includes absorbers selected for the presence of C IV $\lambda\lambda$ 1548.1, 1550.7 resonance-line doublets (Sargent, Steidel, & Boksenberg 1988), Mg II $\lambda\lambda$ 2796.3, 2803.5 resonance-line doublets (Steidel & Sargent 1992) and Lyman limit absorption (Prochaska 1999), which do not also qualify as damped $\text{Ly}\alpha$ systems.

The neutrality of the gas is crucial: while stars are unlikely to form out of warm ionized gas, they are likely to descend from cold neutral clouds, which are the precursors of molecular clouds, the birthplace of stars (Wolfire et al. 2003). This property takes on added significance when it is realized that the damped $\text{Ly}\alpha$ systems dominate the neutral-gas content of the Universe in the redshift interval $z=[0,5]$, and at $z \sim 3.0-4.5$ contain sufficient mass in neutral gas to account for a significant fraction of the visible stellar mass in modern galaxies (e.g. Storrie-Lombardi & Wolfe 2000). This has led to the widely accepted idea that damped

Ly α systems serve as important neutral gas reservoirs for star formation at high redshifts (e.g. Nagamine, Springel, & Hernquist 2004a). Moreover, as repositories of significant amounts of metals the damped Ly α systems have been used to trace the age-metallicity relationship and other aspects of galactic chemical evolution (Pettini et al. 1994; Pei, Fall, & Hauser 1999; Pettini 2004; Prochaska et al. 2003a).

The purpose of this review is to present an overview of the damped Ly α systems. Current research on the high-redshift Universe is dominated by surveys that rely on the detection of radiation emitted by stars (e.g. Steidel et al. 2003; Giavalisco et al. 2004; Dickinson et al. 2003) or ionized gas (e.g. Rhoads & Malhotra 2001; Ouchi et al. 2003). By contrast, damped Ly α systems provide a window on the interplay between neutral gas and newly formed stars, i.e., the damped Ly α systems are the best, perhaps the only, examples we have of an interstellar medium in the high-redshift Universe. Consequently, the focus of this review will be on the manner in which damped Ly α systems trace, and play an active role in, cosmic star formation and hence galaxy formation.

Throughout this article we adopt a cosmology consistent with the *WMAP* (Bennett et al. 2003) results, $(\Omega_m, \Omega_\Lambda, h) = (0.3, 0.7, 0.7)$.

1.1 History of damped Ly α Surveys

To understand the significance of damped Ly α systems for research in galaxy formation we give a brief historical perspective.

The motivation for the first damped Ly α survey was to find the neutral-gas disks of galaxies at high redshifts (Wolfe et al. 1986). Unlike today, the cold dark matter (hereafter CDM) paradigm of hierarchical structure formation (i.e., merging protogalactic clumps) did not dominate theories of galaxy formation in the early 1980s. Rather, the idea of mature galaxy disks at high redshift fitted in with the coherent collapse model of Eggen, Lynden-Bell, & Sandage (1962, also Fall & Efstathiou 1980), which was highly influential at the time. Some QSO absorbers with properties resembling galaxy disks had been found at $z < 1$ through the detection of 21 cm absorption either in radio-frequency scanning surveys (Brown & Roberts 1973) or at the redshifts of Mg II selected absorbers (Roberts et al. 1976). However, application of these techniques resulted in only a few detections. While it was unclear whether the 21 cm absorbers belonged to a new population of objects or were rarely occurring oddities, the radio scanning techniques were valuable for successfully detecting cold, quiescent gas at large redshifts for the first time. Specifically, Brown & Roberts (1973) and Brown & Mitchell (1983) used this technique to detect two 21 cm lines with FWHM velocity widths, $\Delta v_{\text{HI}} \approx 10$ and 20 km s $^{-1}$. The temperature of gas detected in 21 cm absorption is likely to be low, because the 21 cm optical depth $\tau_{21} \propto N(\text{H I})/(T_s \Delta v_{\text{HI}})$, where the hyperfine spin temperature, T_s , generally equals the kinetic temperature of the cold, dense gas detected in 21 cm absorption.

However, the most efficient method for locating quiescent layers of neutral gas is through the detection of damped Ly α absorption lines. In the rest frame of the atom the absorption profile of any atomic transition is naturally broadened owing to the finite lifetime of the upper energy state. In the rest frame defined by the average velocity of the gas, the natural profile is Doppler broadened by the random motions of the atoms: the convolution of both effects results in the Voigt profile (e.g. Mihalas 1978). Because the Doppler profile falls off from the central

frequency, ν_0 , as $\exp[-(\Delta\nu/\Delta\nu_D)^2]$ (where $\Delta\nu = |\nu - \nu_0|$ and $\Delta\nu_D = \sqrt{2}\sigma_v\nu_0/c$ for an assumed Gaussian velocity distribution with dispersion σ_v) and the natural or “damped” absorption profile falls off from ν_0 like $1/(\Delta\nu)^2$, at sufficiently large $\Delta\nu$ the probability for damped absorption exceeds the probability for absorption in the Doppler profile. The frequency intervals in which natural broadening dominates Doppler broadening are called the damping wings of the profile function. Most atomic transitions of abundant ions are optically thin in their damping wings but optically thick near the core of the Doppler profile. The latter transitions have unit optical depth at $\Delta\nu_{\tau=1} \propto \Delta\nu_D \times [\ln N(X^j)]^{1/2}$, where $N(X^j)$ is the column density of ionic species X^j . Such lines are saturated. The reason is that the rest-frame equivalent width of an absorption line is given by $W_r \equiv (\lambda/\nu) \int (1 - \exp(-\tau_\nu)) d\nu$, and therefore W_r is proportional to $\Delta\nu_{\tau=1}$. In the case of lines with unit optical depth near the Doppler core the line is saturated because W_r is insensitive to the value of $N(X^j)$. Due to the higher values of $N(\text{H I})$, Ly α has unit optical depth in the damping wings at $\Delta\nu_{\tau=1} \propto [A_{21}f_{21}N(\text{H I})]^{1/2}$ when $N(\text{H I}) > 10^{19} \text{ cm}^{-2}$ and $\sigma_v < 70 \text{ km s}^{-1}$: A_{21} and f_{21} are the Einstein spontaneous emission coefficient and oscillator strength for the Ly α transition. In this case, unit optical depth occurs in the damping wings, and therefore the equivalent width of a damped Ly α line is independent of the velocity structure of the gas for velocity dispersions within the range detected in most QSO absorption systems. As a result, the equivalent width will be large even when the velocity dispersion is small.

By the early 1980s only four damped Ly α systems had been found. In every case they were high column-density systems, $N(\text{H I}) > 10^{21} \text{ cm}^{-2}$, which were found by chance (Beaver et al. 1972; Carswell et al. 1975; Smith, Margon, & Jura 1979; Wright et al. 1979). Although the sample was sparse, the utility of the damped Ly α criterion was demonstrated when 21 cm absorption at $z \sim 2$ was detected in 2 of the 3 background QSOs that were radio sources (Wolfe & Davis 1979; Wolfe et al. 1981). The narrow line widths, $\Delta\nu_{\text{HI}} \approx 20 \text{ km s}^{-1}$ (where $\Delta\nu_{\text{HI}} = \sqrt{8 \ln 2} \sigma_v$), and relatively low spin temperatures, $T_s < 1000 \text{ K}$, implied that these absorbers were H I layers in which the gas was cold and quiescent.

For these reasons Wolfe et al. (1986) began a survey for damped Ly α systems by acquiring spectra of large numbers of QSOs and then searching them for the presence of damped Ly α absorption lines. The survey for damped Ly α systems had several advantages over surveys for 21 cm absorption lines. For example the redshift interval covered by a single optical spectrum, $\Delta z \approx 1$, is large compared to that sampled by bandpasses then available for 21 cm surveys, $\Delta z \approx 0.02$. Second, optical spectra of QSOs are obtained toward continuum sources with diameters less than 1 pc, whereas the diameters of the associated background radio sources typically exceed 100 pc at the low frequencies of redshifted 21 cm lines. As a result the survey was capable of detecting compact gaseous configurations with low surface covering factors that would have been missed in 21 cm surveys. Another advantage of optical surveys is the large oscillator strength, $f_{21} = 0.418$, of the Ly α transition (by comparison $f_{21} = 2.5 \times 10^{-8}$ times a stimulated emission correction of $0.068 \text{ K}/T_s$ for the 21 cm line), which allows for the detection of warm H I, which is optically thin to 21 cm absorption owing to high values of T_s but optically thick in Ly α . But this is also a disadvantage: the strength of the Ly α transition combined with the high abundance of hydrogen means that the more frequently occurring low column-density clouds in which H is mainly ionized will be optically thick in Ly α . The result is a profusion of Ly α absorption lines,

i.e., the Ly α forest, which dominate the absorption spectrum blueward of Ly α emission (see Figure 1). Although the Ly α forest lines act as excellent probes of the power spectrum and other cosmological quantities (see Tytler et al. 2004; McDonald 2003), they are potential sources of confusion noise for the detection of damped Ly α lines, especially at $z > 4$, since the line density per unit redshift increases with redshift. Identification of damped Ly α lines at $z > 5.5$ is essentially impossible because of Ly α forest confusion noise.

However, at $z < 5.5$ the large column densities of H I in galaxy disks or in any other configuration produce damped Ly α absorption lines that are strong enough to be distinguished from the Ly α forest (see Figure 1). Consider the equivalent widths. At the time of the Wolfe et al. (1986) survey the most accurate 21 cm maps of spiral galaxies were obtained with the Westerbork radio interferometer. These showed the H I column densities of galaxy disks to decrease from $N(\text{H I}) \sim 10^{21} \text{ cm}^{-2}$ at their centers to $N(\text{H I}) = 2 \times 10^{20} \text{ cm}^{-2}$ at a limiting radius $R_l = (1.5 \pm 0.5) R_{26.5}$, which was set by the sensitivity available with Westerbork and comparable radio antennas. Here the Holmberg radius, $R_{26.5}$, is the radius at which the B band surface brightness equals $26.5 \text{ mag arcsec}^{-2}$ (Bosma 1981). The rest-frame equivalent width of a damped Ly α line created by an H I column density, $N(\text{H I})$, is given by $W_r \approx 10 \times [N(\text{H I}) / 2 \times 10^{20} \text{ cm}^{-2}]^{1/2} \text{ \AA}$. Because the observed equivalent width of a line formed at redshift z is $W_{obs} = (1+z)W_r$, damped Ly α systems with $N(\text{H I}) \geq 2 \times 10^{20} \text{ cm}^{-2}$ will appear in optical QSO spectra with $W_{obs} \geq 16 \text{ \AA}$ for damped Ly α systems redshifted redward of the atmospheric cut-off (i.e. $z > 1.6$ for $\lambda_{atm} = 3200 \text{ \AA}$). Lines this strong are easily distinguishable from the $W_{obs} \approx 3 \text{ \AA}$ equivalent widths of typical Ly α forest lines. Furthermore, they can be detected at low resolution and moderate signal-to-noise ratio. Since the goal of the first survey for damped Ly α systems was to find absorbers with $N(\text{H I}) \geq 2 \times 10^{20} \text{ cm}^{-2}$, a spectral resolution, $\Delta\lambda = 10 \text{ \AA}$, was sufficient for resolving candidate features.

1.2 Modern Surveys and Identification of damped Ly α systems

Since the initial survey was published, nine more surveys have been completed for damped Ly α systems with $N(\text{H I}) \geq 2 \times 10^{20} \text{ cm}^{-2}$ (Lanzetta et al. 1991; Lanzetta, Wolfe, & Turnshek 1995; Wolfe et al. 1995; Storrie-Lombardi & Wolfe 2000; Rao & Turnshek 2000; Ellison et al. 2001; Péroux et al. 2003b; Prochaska & Herbert-Fort 2004; Prochaska, Herbert-Fort, & Wolfe 2005). The identification of damped Ly α systems is more complex than for other classes of QSO absorbers. The Ly α forest "clouds", which dominate the absorption spectrum blueward of Ly α emission, are abundant and easy to identify. Similarly, surveys for C IV or Mg II absorption systems rely on the detection of doublets with known wavelength ratios, which are straightforward to locate redward of Ly α emission. By contrast, the task of surveys for damped Ly α systems is to pick out a single damped Ly α line from the confusion noise generated by the Ly α forest. In particular, one must distinguish a single, strong Ly α absorption line created in high column-density gas with low velocity dispersion, but broadened by radiation damping, from strong Ly α absorption features that are Doppler-broadened blends of several lines arising from redshift systems with low column-density gas. The presence of narrow Ly α forest absorption lines in the damping wings of the absorption profile is a further complication which can distort the shape of the true line profile in data of moderate or low signal-to-noise ratios (see Figure 2 for examples).

The most widely used strategy for discovering damped Ly α systems was first introduced by Wolfe et al. (1986) and later refined by Lanzetta et al. (1991) and Wolfe et al. (1995). First, a continuum is fitted to the entire QSO spectrum blueward of Ly α emission. Then damped Ly α candidates are identified as absorption features with rest equivalent widths W_r exceeding $W_{thresh} = 5\text{\AA}$. This conservative criterion corresponds to $N(\text{H I}) \geq 5 \times 10^{19} \text{cm}^{-2}$, which guarantees that few systems with $N(\text{H I})$ above the completeness limit of $2 \times 10^{20} \text{cm}^{-2}$ will be missed. The search is carried out in the redshift interval $z = [z_{min}, z_{max}]$ where z_{min} generally corresponds to the shortest wavelength for which $\sigma(W_r) < 1\text{\AA}$ and z_{max} is set 3000 km s^{-1} below z_{em} to avoid contamination by the background QSO. Finally, a Voigt profile is fitted to the Ly α profile to determine the value of $N(\text{H I})$. Where possible, the centroid is identified from the redshift determined by metal lines outside the Ly α forest. This is particularly important at $z > 3$ where line-blending from the Ly α forest often contaminates the damping wings (e.g. Figure 2). The surveys were time consuming because the signal-to-noise and resolution of the spectra used to acquire damped Ly α system candidates were usually inadequate for fitting Voigt profiles to the data. Therefore, follow-up spectroscopy at higher spectral resolution and with longer integration times was usually necessary.

Recently Prochaska & Herbert-Fort (2004) and Prochaska, Herbert-Fort, & Wolfe (2005) have streamlined this process in a survey based on a single set of QSO spectra drawn from the Sloan SDSS archive (Abazajian et al. 2003). Because of the high quality, good spectral resolution ($R \sim 2000$) and extended spectral coverage of the data, the authors could fit accurate Voigt profiles to the same data used to find damped Ly α system candidates. The authors also bypass the time-consuming step of fitting a continuum to the QSO spectrum blueward of Ly α emission by searching for damped Ly α system candidates in spectral regions with lower-than-average signal-to-noise ratios; i.e., regions coinciding with broad absorption troughs. The survey is not formally complete to $N(\text{H I}) = 2 \times 10^{20} \text{cm}^{-2}$, but the similarity between dN/dX , the number of damped Ly α systems encountered per unit absorption distance along the line of sight (see § 2.1), in their survey and previous surveys suggests they are more than 95% complete. The number of damped Ly α systems for the SDSS DR2 and DR3 archives is 525. As a result the number of damped Ly α systems in a statistically complete sample now exceeds previous samples by an order of magnitude at $z \sim 3$ and several times at $z \sim 4$.

While the H I selection methods are successful at finding damped Ly α systems at $z > 1.6$, they have been unsuccessful at finding large numbers of objects at lower redshifts. This is partly due to the reduced interception probability per unit redshift at low z and partly because few QSOs have been observed from space at UV wavelengths, which is required to detect Ly α at $z < 1.6$. To increase the number of low-redshift damped Ly α systems from the two confirmed objects detected in previous H I selected surveys (see Lanzetta et al. 1995), Rao & Turnshek (2000) searched for damped Ly α systems in samples of QSO absorption systems selected for Mg II $\lambda\lambda$ 2796.3, 2803.5 absorption. Since Mg II absorption is present in every damped system in which it could be observed, it turns out to be a reliable indicator for the presence of damped Ly α . Using this technique, Rao, Turnshek, and collaborators have recently increased the sample size to 41 damped Ly α systems with $z < 1.6$ (SM Rao, DA Turnshek, & DB Nestor 2004, priv. comm.).

The current sample of damped Ly α systems that are drawn from surveys with statistically complete selection criteria comprises over 600 redshift systems. While the number of damped Ly α systems is smaller than the ≈ 2350 objects comprising the population of known Lyman Break galaxies (Steidel et al. 2003), we expect the damped Ly α system population to approach this number when all QSO spectra from the Sloan database become available.

1.3 The Significance of the $N(\text{H I}) \geq 2 \times 10^{20} \text{ cm}^{-2}$ Survey Threshold

The survey statistics cited above refer only to systems with $N(\text{H I}) \geq 2 \times 10^{20} \text{ cm}^{-2}$, which is an historical threshold set by the H I properties of nearby spiral galaxies (see § 1.1). Because the nature of damped Ly α systems is still not understood, their H I properties may differ from those of nearby H I disks: for example, CDM cosmogonies envisage damped Ly α systems as merging protogalactic clumps (Haehnelt, Steinmetz, & Rauch 1998). As a result, it is reasonable to ask whether the $2 \times 10^{20} \text{ cm}^{-2}$ threshold is the appropriate one. Indeed, since the empirically determined frequency distribution of H I column densities increases with decreasing $N(\text{H I})$ (see Figure 3), lower H I thresholds would be advantageous because they would result in larger samples.

Fortuitously, the $2 \times 10^{20} \text{ cm}^{-2}$ threshold is optimal for physical reasons unrelated to the properties of galaxy disks. Rather, at large redshifts this is the column density which divides neutral gas from ionized gas: at $N(\text{H I}) < 2 \times 10^{20} \text{ cm}^{-2}$ the gas is likely to be ionized while at $N(\text{H I}) > 2 \times 10^{20} \text{ cm}^{-2}$ it is likely to be neutral. The minimal source of ionization is background radiation due to the integrated population of QSOs and galaxies. Using background intensities computed by Haardt & Madau (1996, 2003), Viegas (1995) and Prochaska & Wolfe (1996) show that the gas in most of the “sub-damped Ly α ” population (defined to have $10^{19} < N(\text{H I}) < 2 \times 10^{20} \text{ cm}^{-2}$) described by Péroux et al. (2002, 2003a) is in fact significantly ionized with temperature, $T > 10^4$ K. This is a problem since gas neutrality is a necessary condition if damped Ly α systems are to serve as neutral gas reservoirs for star formation at high redshift, a defining property of the population. For this reason the comoving density of H I comprising the sub-damped Ly α population discussed by Péroux et al. (2003b) should not be included in the census of gas available for star formation. As a result, the sub-damped Ly α correction to the comoving density of *neutral* gas, $\Omega_g(z)$, should be ignored. We suggest that these ionization levels make “super Lyman-limit system” a more appropriate name for systems with $10^{19} < N(\text{H I}) < 2 \times 10^{20} \text{ cm}^{-2}$.

2 THE NEUTRAL GAS CONTENT OF THE UNIVERSE

In this section we describe how the surveys allow us to measure $\Omega_g(z)$, the mass per unit comoving volume of neutral gas in damped Ly α systems at redshift z divided by the critical density, ρ_{crit} . The results, first derived by Wolfe (1986) and Lanzetta, Wolfe, & Turnshek (1995) show that damped Ly α systems contain most of the neutral gas in the Universe at redshifts $1.6 < z < 5.0$.

2.1 Formalism

To estimate $\Omega_g(z)$ we first derive an expression for the column density distribution, $f(N, X)$. Let the number of absorbers per sightline with H I column

densities and redshifts in the intervals $(N, N + dN)$ and $(z, z + dz)$ be given by

$$d\mathcal{N}(N, z) = n_{co}(N, z)A(N, z)(1 + z)^3|cdt/dz|dNdz \quad , \quad (1)$$

where $n_{co}(N, z)dN$ is the comoving density of absorbers within $(N, N + dN)$ at z and $A(N, z)$ is the absorption cross section at (N, z) . Defining $dX \equiv (H_0/c)(1 + z)^3|cdt/dz|dz$ (Bahcall & Peebles 1969) we have

$$\frac{d\mathcal{N}(X)}{dX} = \int_{N_{min}}^{N_{max}} dN f(X, N) \quad , \quad (2)$$

where

$$f(N, X) \equiv (c/H_0)n_{co}(N, X)A(N, X) \quad , \quad (3)$$

and where N_{min} and N_{max} are minimum and maximum column densities¹. Therefore, one cannot infer the comoving density nor the area of damped Ly α systems from their incidence along the line of sight, but only their product. Note, $d\mathcal{N}/dX$ will be independent of redshift if the product of the comoving density and absorption cross section at (N, X) is independent of redshift. Since the gaseous mass per damped Ly α system is given by $\mu m_H N A(N, X)$, it follows from eq. (3) that

$$\Omega_g = \frac{H_0 \mu m_H}{c \rho_{crit}} \int_{N_{min}}^{N_{max}} dN N f(N, X) \quad . \quad (4)$$

where μ is the mean molecular weight, which is included to account for the contribution of He to the neutral gas content.

Using these expressions in the discrete limit, several authors have determined $f(N, X)$ and its first two moments, $d\mathcal{N}/dX$ and $\Omega_g(z)$, where

$$\Omega_g(X) = \frac{H_0 \mu m_H}{c \rho_{crit}} \frac{\sum_{i=1}^n N_i}{\Delta X} \quad , \quad (5)$$

and n is the number of damped Ly α systems within $(X, X + \Delta X)$. We now discuss each of these in turn.

2.2 $f(N, X)$

Figure 3 shows the most recent determination of $f(N, X)$ from the statistical sample of over 600 damped Ly α systems (Prochaska, Herbert-Fort, & Wolfe 2005). The figure also shows best-fit solutions for the three functional forms used to describe $f(N, X)$: a single power-law, $f(N, X) = k_1 N^{\alpha_1}$; a Γ function (e.g. Pei & Fall 1993) $f(N, X) = k_2 (N/N_\gamma)^{\alpha_2} \exp(-N/N_\gamma)$; and a double power-law $f(N, X) = k_3 (N/N_\gamma)^\beta$ where $\beta = \alpha_3$ at $N < N_d$ and α_4 at $N \geq N_d$. The single power-law solution with a best-fit slope of $\alpha_1 = -2.20 \pm 0.05$ is a poor description of the data since a KS test shows there is a 0.1% probability that the data and power-law solution are drawn from the same parent population. This result is in contrast with the Ly α forest where a single power-law with $\alpha_1 \approx -1.5$ provides a good fit to the data (Kirkman & Tytler 1997).

Although a single power-law is a poor fit to the observations, the $f(N, X)$ distribution is steeper than N^{-2} at large column densities. This is illustrated by the other two curves in Figure 3 that show the Γ function (dashed line) and

¹Note that $dX/dz = (1 + z)^2[(1 + z)^2(1 + z\Omega_m) - z(z + 2)\Omega_\Lambda]^{-1/2}$

the double power-law (dashed-dot line). Both solutions are good fits to the data. Furthermore, the solutions provide good agreement between the ‘break’ column densities N_γ and N_d , and between the power-law indices at low column densities, which approach a ‘low-end’ slope $\alpha = -2.0$. Most importantly, both solutions indicate $\alpha \ll -2.0$ at $N \geq 10^{21.5} \text{ cm}^{-2}$: the significance of this very steep slope at the ‘high end’ will be explored further in § 2.4.

Prochaska, Herbert-Fort, & Wolfe (2005) also find evidence for evolution in $f(N, X)$, which will be clearly visible in the redshift dependence of dN/dX , the zeroth moment of $f(N, X)$, and of $\Omega_g(z)$, the first moment of $f(N, X)$ (see § 2.3 and § 2.4). At low column densities, $f(N, X)$ increases with redshift by a factor of 2 at $z \geq 2.2$. Prochaska, Herbert-Fort, & Wolfe (2005) detect a similar evolution at higher values of N . By contrast the shape of $f(N, X)$ does not appear to evolve with redshift. This is in disagreement with the earlier results of Storrie-Lombardi & Wolfe (2000) and Péroux et al. (2003b) who used much smaller samples to claim that $f(N, X)$ steepened at $z > 3.5$.

2.3 dN/dX

In Figure 4 we plot the most recent evaluation of dN/dX versus z for damped Ly α systems with $z \geq 0$ (see Prochaska, Herbert-Fort, & Wolfe 2005). The solid line traces the value of dN/dX derived in a series of 0.5 Gyr time intervals to reveal the effects of binning. The data points at $z = 0$ are three estimates of $(dN/dX)_{z=0}$ based on the H I properties of nearby galaxies. The figure shows a decrease by a factor of two in dN/dX from $z=4$ to 2. From equations 2 and 3 we see that the decrease in dN/dX reflects a decrease in either H I cross section, comoving density, or of both quantities. Prochaska, Herbert-Fort, & Wolfe (2005) use the Press-Schechter formalism to show that significant variations in comoving density with time are unlikely to occur. Therefore, within the context of CDM models the most likely explanation for the changes in dN/dX is a decrease in H I cross section with time. This is probably due to feedback mechanisms such as galactic winds.

Figure 4 also shows that dN/dX at $z \approx 2$ is consistent with the present-day value; i.e., the data are consistent with an unevolving population of galaxies². By comparison, Wolfe et al. (1986) required more than a factor of 4 increase with redshift in dN/dX . The discrepancy arises from the earlier use of an Einstein-deSitter rather than the modern Λ CDM cosmology to estimate ΔX intervals, and from the lower values of $(dN/dX)_{z=0}$ used in the earlier work. This result implies that between $z = 1$ and 2 smaller galaxies merged to produce bigger ones such that the product of comoving density and total H I cross-section for $N(\text{H I}) \geq 2 \times 10^{20} \text{ cm}^{-2}$ is conserved.

2.4 $\Omega_g(z)$

Figure 5 shows the most recent determination of $\Omega_g(z)$. From Equation (4) we see that $\Omega_g(z)$ is sensitive to the upper limit N_{max} unless $\alpha \ll -2$. This led to large uncertainties in $\Omega_g(z)$ in previous work because α was not measured

²Ryan-Weber, Webster, & Staveley-Smith (2003) present evidence that $f(N, X)$ at $z=0$ is significantly lower in amplitude than the results at higher redshifts, but this result is puzzling since comparison between the resultant dN/dX at $z=0$ with the higher redshift data in Figure 4 reveals no evidence for evolution.

with sufficient accuracy to rule out $\alpha \geq -2$. However, with the large sample of over 600 damped Ly α systems Prochaska, Herbert-Fort, & Wolfe (2005) use several tests to show that $\Omega_g(z)$ converges. First, they compute α_1 for a single power-law fit to $f(N, X)$ by increasing N_{min} from $2 \times 10^{20} \text{ cm}^{-2}$. Using the full sample of damped Ly α systems they find α_1 decreases with increasing N_{min} from -2.2 at $N_{min} = 2 \times 10^{20} \text{ cm}^{-2}$ to less than -3 at $N_{min} > 10^{21} \text{ cm}^{-2}$. At the same time they find that α_1 is insensitive to variations in N_{max} . Second, they compute the sensitivity of $\Omega_g(z)$ to N_{max} . Both the double power-law and Γ function solutions converge to the value indicated by the data (Equation 5). By contrast the single power-law solution does not converge. This is the first evidence that $\Omega_g(z)$ converges by $N \approx 10^{22} \text{ cm}^{-2}$.

Next consider the redshift evolution of $\Omega_g(z)$. Starting at the highest redshifts, no increase of $\Omega_g(z)$ with decreasing z is present at $z > 3.5$, contrary to earlier claims (Storrie-Lombardi & Wolfe 2000; Péroux et al. 2003b). On the other hand, Figure 5 shows the first statistically significant evidence that $\Omega_g(z)$ evolves with redshift. Specifically, $\Omega_g(z)$ decreases from 1×10^{-3} at $z=3.5$ to 0.5×10^{-3} at $z=2.3$, which mirrors the decline in dN/dX discussed in § 2.3. The same mechanism is likely to cause the decline in both quantities; i.e., a decrease in H I cross section due to feedback. But at $z < 2.3$ the picture is somewhat confusing. Figure 5 shows an *increase* of $\Omega_g(z)$ by $z \sim 2$, which is consistent with the values of $\Omega_g(z)$ in the two lower redshift bins at $0 < z < 2$. Indeed, the data are consistent with no evolution, if one ignores the redshift interval centered at $z = 2.3$. However, Prochaska, Herbert-Fort, and Wolfe (2005) emphasize that the uncertainties in the data at $0 < z < 2.3$ are much larger than at $z > 2.3$, and thus such conclusions should be treated with caution.

Next, we compare the high- z values of $\Omega_g(z)$ with various mass densities at $z = 0$. First, comparison with the current density of visible stars, $\Omega_*(z = 0)$, reveals that $\Omega_g(z)$ at $z \approx 3.5$ is a factor of 2 to 3 lower than $\Omega_*(z = 0)$: if the census of visible stars were restricted to stellar disks, then $\Omega_g(z)$ at these redshifts would exceed $\Omega_*(z = 0)$. A straightforward interpretation of this concurrence is that damped Ly α systems provide the neutral gas reservoirs for star formation at high redshifts. However, since $\Omega_*(z = 0)$ exceeds $\Omega_g(z \approx 3.5)$, the reservoir must be replenished with new neutral gas before the present epoch. Further evidence for replenishment is that it is required to compensate for gas depletion due to star formation detected in damped Ly α systems (see § 8). As a result the “closed box” hypothesis for evolution in damped Ly α systems is unlikely to be correct (see Lanzetta et al. 1995).

Figure 5 also shows that $\Omega_g(z)$ at $z \approx 3.5$ is significantly higher than $\Omega_g(z)$ at $z = 0$, which is deduced from surveys for 21 cm emission. Therefore, damped Ly α systems provide direct evidence for the widely held theoretical view that the neutral gas content of the Universe was larger at high redshifts than it is today. Figure 5 also shows that $\Omega_g(z)$ at $z \approx 3.5$ is at least a factor of 10 greater than $\Omega_*(z = 0)$ in dwarf irregular galaxies, which argues against the idea that damped Ly α systems evolve into such objects (e.g. Jimenez et al. 1999).

Therefore, since Lyman limit systems do not contribute significantly to the *neutral* gas content at any redshift (see Prochaska, Herbert-Fort, & Wolfe 2005) and ignoring the possible existence of a significant population of dusty giant molecular clouds, we conclude that damped Ly α systems contain most of the gas available for star formation at $z > 1.6$. At low redshifts the ionizing background is reduced and lower $N(\text{H I})$ systems might be mainly neutral. But at $z = 0$,

Minchin et al. (2003) find a paucity of galaxies with column densities less than $N(\text{H I}) = 2 \times 10^{20} \text{ cm}^{-2}$ measured from 21cm emission, implying that at the lowest redshifts, damped Ly α system column densities comprise most of the neutral gas in the Universe. As a result, damped Ly α systems dominate the neutral-gas content of the Universe in the redshift interval $z = [0, 5]$.

Of course, all of these conclusions ignore obscuration by dust in damped Ly α systems, which may have biased the form of $f(N, X)$ (see Pei, Fall, & Bechtold 1991; Fall & Pei 1993). We discuss this possibility in § 10. They also ignore biasing due to lensing, which may be present (see § 11).

2.5 Model Comparisons

Here we discuss attempts to use the H I content of damped Ly α systems to test models of galaxy formation and evolution.

2.5.1 Passive Evolution: The Null Hypothesis

The evolution of H I content within the null hypothesis of passive evolution has been modeled by Boissier, Péroux, & Pettini (2003). In this scenario damped Ly α absorption arises in disk galaxies with the comoving density of current spiral galaxies. The models are hybrids of passive evolution, in which the H I content is changed only by processes of stellar evolution, and the spherical collapse model in an expanding Universe, in which high- z disks are smaller than current disks. The models are successful in explaining the lack of evolution in dN/dX , $f(N, X)$, and $\Omega_g(z)$ at $z < 2$ but fall short at higher redshifts because of delayed disk formation. For these reasons, the authors suggest the added presence of a population of low-surface brightness, gas-rich galaxies at $z > 2$. However, evidence against the “closed box” hypothesis discussed in § 2.4 is a difficult challenge for this and all passive evolution models.

2.5.2 Numerical Simulations

Several aspects of cosmology and galaxy formation have been examined through comparisons of numerical simulations of galaxy formation in a CDM Universe with the observed H I properties of damped Ly α systems. A critical feature of these models is that gas falling onto dark-matter halos is heated to their virial temperatures, then cools off, and collapses toward the central regions of the halos. Galaxies arise from the formation of stars out of the cool (presumably neutral) collapsed gas and evolve through mergers between dark-matter halos and further infall of gas onto the halos.

The first studies (Ma & Bertschinger 1994; Klypin et al. 1995) constrained the cosmological mass constituents through comparisons with $\Omega_g(z)$. The observations severely restricted the contribution from a hot component (i.e. neutrinos) as these cold+hot dark matter cosmogonies underpredicted structure formation at early times (Katz et al. 1996). Subsequent papers by Gardner et al. (1997a,b, 2001) examined the properties of damped Ly α systems in their smooth particle hydrodynamic (SPH) simulations. These models generically underpredicted the incidence of damped Ly α systems, which the authors argued was due to an insufficient mass resolution of $10^{11} M_\odot$. They did find reasonable agreement with the data, however, by extrapolating to halos with $M_h > 10^{10} M_\odot$ using the

Press-Schechter formalism, and by assuming that the HI cross-section followed the power-law expression $A \propto v_c^{1.6}$. As stressed by Prochaska & Wolfe (2001), this power-law expression implies a v_c distribution that is incompatible with the observed damped Ly α velocity widths (see § 6).

Nagamine, Springel, & Hernquist (2004a) recently analyzed a comprehensive set of high resolution SPH simulations of a Λ CDM Universe. By contrast with Gardner et al. (1997a) they find that halo masses down to $M_h \approx 10^8 M_\odot$ contribute to the HI cross-sections: halos with $M_h < 10^8 M_\odot$ do not contribute since they contain only photo-ionized gas. In turn, Nagamine et al. find a steeper power-law expression $A \propto v_c^{2.7}$, i.e., massive halos make a larger contribution to dN/dX than in previous models. They conclude that Gardner et al. (1997a) predicted an overabundance of damped Ly α systems with $M_h < 10^{10} M_\odot$ because the slope of their A versus v_c relation was too shallow. Nagamine, Springel, & Hernquist (2004a) were the first to include mass loss of neutral gas due to winds, which increases the median halo-mass contribution to dN/dX to $10^{11} M_\odot$. Winds also prevent an overabundance of $\Omega_g(z)$ at $z > 4$, but underpredict $\Omega_g(z)$ at $z < 4$. Nagamine et al. (2004a) continue to find a deficit of damped Ly α systems with $N(\text{HI}) < 10^{21} \text{ cm}^{-2}$. The deficit of systems with low $N(\text{HI})$ is a generic effect seen in most (e.g. Figure 3 in Katz et al. 1996) but not all numerical simulations (Cen et al. 2003) and is a shortcoming that needs to be addressed. On the other hand, the Nagamine, Springel, & Hernquist (2004a) models are the most successful in reproducing the evolution of $\Omega_g(z)$ at $z > 2$ (see Figure 5).

2.5.3 Semi-analytic and Analytic Models

The semi-analytic models were proposed to include processes beneath the resolution of the numerical simulations with phenomenological descriptions of star formation, gas cooling, and the spatial distribution of the gas. The latter is included since the simulations failed to reproduce the correct sizes and angular momenta of present-day galactic disks (Navarro & Steinmetz 2000), and we do not know whether the simulations produce the correct spatial distribution of neutral gas at $z \sim 3$. This is a concern because damped Ly α systems are a cross-section weighted population of high-redshift layers of neutral gas and therefore the results will be sensitive to the gas distribution at large impact parameters. By contrast with the numerical simulations, one uses analytic expressions from Press-Schechter theory or its extensions (Press & Schechter 1974; Sheth, Mo, & Tormen 2001) to compute the mass function of halos that evolves from a given power spectrum.

Mo & Miralda-Escudé (1994) modeled damped Ly α systems with the Press-Schechter formalism in both mixed Cold+Hot dark matter and Λ CDM cosmologies. Kauffmann (1996) used a SCDM cosmology ($[\Omega_M, \Omega_\Lambda, h] = 1.0, 0.0, 0.5$) to construct improved semi-analytic models for damped Ly α systems. She assumed spherical geometry for the halos and let the neutral gas in a given halo be confined to a smaller, centrifugally supported disk. To compute the radial distribution of the neutral gas, the angular momentum per unit mass of the disk was set equal to that of the halo. Using Monte Carlo methods, she computed the formation and growth of individual halos with time. The neutral gas content was assumed to be regulated by accretion due to mergers and star formation, but feedback due to winds was omitted. In common with the Nagamine, Springel, & Hernquist

(2004a) simulations, the Kauffmann (1996) models (1) reproduced the $\Omega_g(z)$ relation, and (2) exhibited a deficit of systems with $N(\text{H I}) < 10^{21} \text{ cm}^{-2}$.

Mo, Mao, & White (1998) constructed models for disk formation that were also based on the Press-Schechter formalism. These models extended the work of Kauffmann (1996) by considering disks drawn from a distribution of halo spin parameters, λ_H , rather than using Kauffmann’s technique of assigning the mean value of λ_H to each disk. Since disks detected in a survey for damped Ly α systems are drawn from a cross-section weighted sample favoring bigger disks, the distribution of λ_H will be skewed to values higher than the unweighted mean. The result is larger H I cross-sections and higher detected rotation speeds. Consequently, they found agreement between the predicted and observed dN/dX relation. Maller et al. (2001) then suggested a model in which the gas is in extended Mestel (1963) disks in which the surface density falls off inversely with radius. In this case the disks overlap and as a result the observed $f(N, X)$ is reproduced; i.e., there is no deficit of systems with $N(\text{H I}) < 10^{21} \text{ cm}^{-2}$. However, it is unclear whether such extended disks will either form or survive sufficiently long to contribute to the H I cross-sections of damped Ly α systems. Furthermore, most semianalytic models overestimate $\Omega_g(z)$ at $z > 2$, since they underpredict feedback processes at these redshifts (see Figure 5).

3 CHEMICAL ABUNDANCES

Because the damped Ly α systems comprise the neutral gas reservoir for star formation at high redshifts, a determination of their metal content is a crucial step for understanding the chemical evolution of galaxies. Therefore, the mass of metals per unit comoving volume that they contribute indicates the level to which the neutral gas reservoir has been chemically enriched. Since the metal abundances of damped Ly α systems have been determined in the redshift interval $z = [0, 5]$, it is now possible to track the chemical evolution of the reservoir back ≈ 10 Gyr to the time the thin disk of the Galaxy formed ($z = 1.8$ for the WMAP cosmological parameters adopted here), and to earlier epochs. As a result, one can construct an “age-metallicity” relation not just for the solar neighborhood (see Edvardsson et al. 1993) but for a fair sample of galaxies in the Universe.

In this section we describe the main results that have emerged from abundance studies of damped Ly α systems. This subject has recently been reviewed in an excellent article by Pettini (2004).

3.1 Methodology

The element abundances of the damped Ly α systems are the most accurate measurements of chemical enrichment of gas in the high-redshift Universe. The measurements are accurate for several reasons: (1) For the majority of damped Ly α systems, hydrogen is mostly neutral, i.e., $\text{H}^0/\text{H}=1$, and most of the abundant elements are singly ionized, though a minority are neutral, i.e., $\text{Fe}^+/\text{Fe}=\text{Si}^+/\text{Si}=1$, etc., while $\text{O}^0/\text{O}=\text{N}^0/\text{N}=1$. The singly ionized elements have ionization potentials of their neutral states that are lower than the ionization potential of hydrogen, $\text{IP}(\text{H}) (=13.6 \text{ eV})$. With Lyman limit optical depths, $\tau_{LL} \gg 10^3$, damped Ly α systems are optically thick at photon energies, $\text{IP}(\text{H}) \leq h\nu \leq 400 \text{ eV}$. As a result, only photons with $h\nu \leq \text{IP}(\text{H})$ and $h\nu \geq 400 \text{ eV}$ penetrate deep into the neutral gas. When FUV photons with $h\nu \leq \text{IP}(\text{H})$ penetrate, they photoionize

the neutral state of each element to the singly ionized state. But this state is shielded from photons with $\text{IP}(\text{H}) \leq h\nu \leq 400 \text{ eV}$, which would otherwise photoionize the elements to higher states. Photons with $h\nu > 400 \text{ eV}$ will produce species that are doubly ionized (e.g. Fe^{++} and Al^{++}) and singly ionized (e.g. Ar^+), but because the photoionization cross-sections are low at such high photon energies, the ionization rates are low. It is possible to detect all of these species because they exhibit resonance transitions that are redshifted to optical wavelengths accessible with ground based spectrographs. (2) In § 1 we saw that Voigt fits to the damped $\text{Ly}\alpha$ profiles result in typical errors of 0.1 dex in $N(\text{H I})$. As we shall see, the errors in the column densities which give rise to the narrow low-ion lines are typically 0.05 dex. Consequently, errors in $[\text{X}/\text{H}]$ ³ are relatively low (typically about 0.1 dex). (3) Column densities are straightforward to measure from resonance lines, since their optical depths are independent of poorly determined physical parameters such as the density and temperature of the absorbing gas.

By contrast, abundance determinations for the other constituents of the high-redshift Universe are more uncertain primarily because the gas is ionized. As a result, the abundances are subject to ionization corrections which depend on uncertainties in the shape of the ionizing continuum radiation and on the transport of such radiation. Furthermore, the strengths of QSO emission lines depend on the temperature and density of the emitting gas as well as uncertain photon escape probabilities in the case of resonance scattering. Typical error estimates are about 50 % per object, which is several times higher than for damped $\text{Ly}\alpha$ systems (see Hamann & Ferland 1999 for an excellent review of this subject).

Figure 6 shows examples of absorption profiles obtainable with the HIRES Echelle spectrograph mounted on the Keck I 10-m telescope. The figure shows velocity profiles for abundant low ions in two damped $\text{Ly}\alpha$ systems. As in most damped $\text{Ly}\alpha$ systems the gas that gives rise to low-ion absorption lines in these two objects is comprised of multiple discrete velocity structures of enhanced density; i.e., clouds. To infer the ionic column densities required for element abundance determinations, one integrates the “apparent optical depth” (Savage & Sembach 1991; Jenkins 1996) over the velocity profile.

To illustrate the essentials of abundance determinations we focus on two damped $\text{Ly}\alpha$ systems, one metal-poor (DLA1108–07 at $z = 3.608$) and the other metal-rich (DLA0812+32 at $z = 2.626$)⁴. The corresponding velocity profiles in Figure 6 describe the challenges as well as the advantages of measuring damped $\text{Ly}\alpha$ abundances. First consider the challenges. The abundance of carbon has not been accurately determined for any damped $\text{Ly}\alpha$ system because the only resonance transition outside the $\text{Ly}\alpha$ forest, C II $\lambda 1334.5$, is not only saturated in the metal-rich system (Figure 6b), but is also saturated in the metal-poor system (Figure 6a). The availability of several O I transitions makes it possible to place bounds on the oxygen abundance. Several authors used saturated O I $\lambda 1302.1$ to obtain lower limits and the weaker O I $\lambda 971.1$ or O I $\lambda 950.8$ transitions for upper limits since the latter transitions are usually blended with $\text{Ly}\alpha$ forest absorption features (D’Odorico & Molaro 2004; Molaro et al. 2000; Dessauges-Zavadsky, Prochaska, & D’Odorico 2002). On the other hand, a direct

³Here and in what follows the relative abundance of elements X and Y is defined with respect to the solar abundance on a logarithmic scale; i.e. $[\text{X}/\text{Y}] = \log_{10}(\text{X}/\text{Y}) - \log_{10}(\text{X}/\text{Y})_{\odot}$.

⁴Here and in what follows we designate a damped $\text{Ly}\alpha$ system toward a QSO with coordinates hhmm±deg as DLAhmm±deg

determination of [O/H] is possible for the metal-rich system shown in Figure 6b because this is the only known case in which an unsaturated transition, O I λ 1355.6, is detected.

Second consider the advantages. Abundance determinations are possible for Fe, Si, and S because of the presence of transitions with a wide range of oscillator strengths. In the case of Fe, the oscillator strengths $f_{1611.2} = 0.00136$ for Fe II λ 1611.2 and $f_{1608.4} = 0.0580$ for Fe II λ 1608.4. Thus, in the metal-poor damped Ly α system in Figure 6a Fe II λ 1611.2 is undetected, while unsaturated Fe II λ 1608.4 is detected. By contrast, in the metal-rich damped Ly α system in Figure 6b unsaturated Fe II λ 1611.2 is detected, while Fe II λ 1608.4 is saturated. In both systems the iron abundance is determined from the unsaturated transitions. Similarly, Figure 6 also demonstrates how the Si II λ 1304.3, 1808.0 pair of transitions determines the silicon abundance for the two damped Ly α systems.

3.2 Metallicity

Whereas the abundance ratios discussed above refer only to elements in the gas phase, some fraction of each element could be depleted onto dust grains, as in the Galaxy ISM (Jenkins 1987). This possibility was recognized early on by Meyer, Welty, & York (1989) and Pettini, Boksenberg, & Hunstead (1990) who made use of the Zn II $\lambda\lambda$ 2026.1, 2062.6 doublet to measure the metallicities of damped Ly α systems. Zn is well suited for this purpose because Zn is relatively undepleted in the ISM with a mean depletion of [Zn/H] ≈ -0.23 (Savage & Sembach 1996). Moreover Zn was believed to be an accurate tracer of Fe peak elements since [Zn/Fe] ≈ 0 for stars with metallicities, $-2.0 < [\text{Fe}/\text{H}] < 0$ (but see discussion below). In addition the combination of the low solar abundance of Zn and the oscillator strengths of the Zn II transitions implies they should be unsaturated for $N(\text{H I}) \leq 10^{21} \text{ cm}^{-2}$, provided the velocity dispersion of the gas, $\sigma_v \geq 4 \text{ km s}^{-1}$. Because of its proximity in wavelength, the Cr II $\lambda\lambda$ 2056.2, 2062.2, 2066.1 triplet was used to study depletion, since most of the Cr in the ISM is locked up in grains (Jenkins 1987).

In subsequent surveys on several 4 m class telescopes, Pettini and colleagues (Pettini et al. 1994, 1997b, 1999) increased the size of their sample and confirmed that damped Ly α systems are metal-poor in the redshift interval $z = [0.5, 3.0]$. Pettini (2004) found that the cosmic metallicity $\langle Z \rangle = -1.11 \pm 0.38$, where $\langle Z \rangle$ is defined as the log of the ratio of the comoving densities of metals and gas, $\Omega_{\text{metals}}/\Omega_g$, relative to the solar abundance; i.e. from Equation 5

$$\langle Z \rangle = \log_{10} \left[\frac{\sum_{i=1}^n 10^{[\text{M}/\text{H}]_i} N_i}{\sum_{i=1}^n N_i} \right] - \log_{10}(\text{M}/\text{H})_{\odot} \quad , \quad (6)$$

where M stands for the metallicity indicator, which in this case is Zn. Second, surprisingly, there is no positive evidence for redshift evolution. Specifically, Pettini (2004) finds no statistically significant evidence for redshift evolution in $\langle Z \rangle$. This is contrary to most models of chemical evolution (see § 9), which predict an increase in the mean Zn abundance with decreasing redshift, and further predict that the metallicity should approach $\langle Z \rangle = 0$, by the current epoch. The sub-solar values of $\langle Z \rangle$ at $z < 1$ raised the possibility that damped Ly α systems do not evolve into normal current galaxies (Pettini et al. 1999).

Further progress was achieved with the completion of a larger survey of over 120 damped Ly α systems carried out primarily on the Keck 10-m telescopes

(Prochaska et al. 2003a). In this survey most of the metallicities, $[M/H]$, are obtained from measurements of α -enhanced elements Si, S, and O in order of decreasing priority and in a few cases from Zn. Like Zn, S and O are volatile elements which are essentially undepleted in the ISM. While the refractory element Si is depleted in the ISM, it is only mildly depleted in damped Ly α systems, where Si tracks S, i.e., $[Si/S] > -0.1$ (Prochaska & Wolfe 2002), and thus can generally be used as an unbiased metallicity tracer. Furthermore, since S and Si have higher solar abundances than Zn, they can be used to probe down to metallicities below the Zn threshold of $[Zn/H] \approx -1.7$. In addition, the shorter wavelengths of crucial transitions such as S II λ 1250.5 and Si II λ 1304.3 allow one to obtain metal abundances at higher redshifts than are accessible with the Zn II transitions alone. Note, the idea of combining abundances of Zn and α -enhanced elements is plausible if Zn is a tracer of elements such as S, Si, etc. The recent finding by Prochaska & Wolfe (2002) that $[Si/Zn] = 0.03 \pm 0.05$ supports this hypothesis. Further support comes from the finding that $[Zn/Fe]$ ranges between 0.10 to 0.20 (Prochaska et al. 2000; Nissen et al. 2004; Bihain et al. 2004) in stars with $[Zn/H] > -1.5$, which indicates Zn is not a strict tracer of Fe peak elements. In fact there is currently little reason to expect $[Zn/Fe]=0$ aside from a coincidence related to the star formation history of the Galaxy (Fenner, Prochaska, & Gibson 2004).

The results of Prochaska et al. (2003a) are shown in Figure 7 (updated to include new data at $z < 1.5$ from Kulkarni et al. 2005 and Rao et al. 2005). The new survey confirms the low metallicities of damped Ly α systems found by Pettini and colleagues. However, the greater accuracy and larger redshift range of the new survey allows one to draw additional conclusions. First, there are no damped Ly α systems with $[M/H] < -2.6$. This limit is robust because there are no damped Ly α systems without significant metal absorption. Second, Prochaska et al. (2003a) find statistically significant evidence for a linear increase of $\langle Z \rangle$ with decreasing z . This result is robust owing to the large value of $\sum_i^m N_i$. This is important since the shape of $f(N, X)$ indicates that $\langle Z \rangle$ is sensitive to the metallicity of systems with the largest values of $N(\text{H I})$. Because $\sum_i^m N_i > 1 \times 10^{22} \text{ cm}^{-2}$ in each of the high-redshift bins, only unusual, very metal-rich systems with $N(\text{H I}) > 10^{22} \text{ cm}^{-2}$ could increase $\langle Z \rangle$ significantly; i.e., only systems which depart significantly from the current $N(\text{H I})$ versus $[M/H]$ relation could cause a marked increase in $\langle Z \rangle$. Earlier claims for evolution had statistical significance lower than 3σ and sampled lower values of $\sum_i^n N_i$ (Kulkarni & Fall 2002; Vladilo 2002b).

The “age-metallicity” relationship depicted in Figure 7 provides new information about the enrichment history of damped Ly α systems. Specifically, the absence of any system with a metallicity $[M/H] < -2.6$ sets the damped Ly α systems apart from the Ly α forest. From their analysis of the Ly α forest, Simcoe, Sargent, & Rauch (2004) find a median abundance, $[C, O/H] = -2.8$ and find that 30 % of their sample have $[C, O/H] < -3.5$. Schaye et al. (2003) find similar results for $[C/H]$. While they deduce a higher median abundance for Si, i.e., $[Si/H] = -2.0$, about 40 % of their systems are predicted to have $[Si/H] < -2.6$. Clearly the bulk of the damped Ly α population has a different enrichment history than the Ly α forest. To explain the presence of the metallicity floor, Qian & Wasserburg (2003) use a standard chemical evolution model to show that star formation in damped Ly α systems results in a rise in metal abundance which is so rapid that the probability for detecting systems with $[M/H] < -2.6$ is exceedingly

small.

Figure 7 also poses several dilemmas for models of chemical evolution. First, if most of the gas in damped Ly α systems in the redshift interval $z = [1.6, 4.5]$ were converted into stars, then most of the stellar mass in current galaxies would be metal poor, contrary to observations Tremonti et al. (2004). Second, the age-metallicity relation of the thin disk of the Galaxy (Edvardsson et al. 1993), indicates that the thin disk formed at lookback times less than 10 Gyr (i.e., $z \approx 1.8$) and that chemical enrichment proceeded such that *all* thin disk stars formed with $[M/H] > -1.0$. But the lower panel in Figure 7 shows that $[M/H] < -1.0$ in about half of the damped Ly α systems with look-back times under 10 Gyr. While this result is subject to the uncertainties of small number statistics and observational bias, the current metallicity trends in low-redshift damped Ly α systems suggest that damped Ly α systems may not trace the star formation history of normal galaxies (Pettini et al. 1999). Third, if the linear increase of $\langle Z \rangle$ with decreasing redshift deduced at $z > 1.6$ is extrapolated to $z = 0$, the current mean metal abundance of galaxies would be equal to -0.69 which appears too low. But since the age-metallicity relationship is essentially unconstrained by the data at $z < 1.6$, such extrapolations should be treated with caution. Indeed, $\langle Z \rangle$ is doubling every Gyr at $z > 2$, and if we assumed $\langle Z \rangle$ to be a linear function of *time* rather than redshift, then we would find that $\langle Z \rangle \approx 0$ by $z \approx 0.5$.

3.3 Relative Abundances

In § 3.2 we described evidence that damped Ly α systems are metal-poor. We discussed measurements of Zn and Cr which indicate a gas-phase abundance ratio, $[Zn/Cr] > 0$, implying depletion of Cr by dust. Since metal-poor stars in the Galaxy exhibit different nucleosynthetic abundance ratios than the sun (Wheeler, Sneden, & Truran 1989), the abundance patterns observed in damped Ly α systems are probably due to some combination of nucleosynthetic and dust depletion patterns. In this section we briefly describe efforts to unravel these effects. The reader is referred to a series of recent papers for a more thorough discussion of these issues (Prochaska & Wolfe 2002; Vladilo 2002b; Pettini 2004).

3.3.1 Depletion

The discussions of metallicity in the previous subsections implicitly assumed that deviations of $(X/H)_{gas}$, the gas-phase abundance of element X, from the solar abundance, $(X/H)_{\odot}$, were only due to changes in the intrinsic abundance, $(X/H)_{int}$. However, as mentioned previously, $(X/H)_{gas}$ will also deviate from $(X/H)_{\odot}$ if element X is depleted onto grains. One of the major challenges in damped Ly α research is to untangle these two effects.

The traditional method used by most workers in the field is to compare the abundance of refractory element, X, to volatile element, Y, for which $(X/Y)_{int} = (X/Y)_{\odot}$ in stars with a wide range of absolute abundances. In that case the condition $[X/Y] \neq 0$ is unlikely to have a nucleosynthetic origin. Rather it likely arises from depletion of the refractory element onto grains. Such a comparison is made in Figure 8a, which is a plot of $[Zn/Fe]$ versus $[Zn/H]$ for a sample of 32 damped Ly α systems. The figure reveals an unambiguous correlation between $[Zn/Fe]$ and $[Zn/H]$: a Kendall τ test rules out the null hypothesis of no cor-

relation at more than 99.7 % confidence. Because $[\text{Zn}/\text{Fe}] < 0.2$ for Galactic stars with $[\text{Fe}/\text{H}] > -2.0$, the most plausible explanation for this correlation is that in damped Ly α systems the depletion of Fe onto grains increases with metal abundance. This argument also suggests that the depletion level decreases with decreasing metal abundance. In that case $[\text{Zn}/\text{Fe}]$ should approach the intrinsic nucleosynthetic ratio, $[\text{Zn}/\text{Fe}]_{\text{int}}$, in the limit $[\text{Zn}/\text{H}] \ll 0$. Determination of $[\text{Zn}/\text{Fe}]_{\text{int}}$ is important as it indicates the nucleosynthetic history of these elements (Hoffman et al. 1996), and it is required for determining the dust-to-gas ratio, κ . For example, Wolfe, Prochaska, & Gawiser (2003b) show that

$$\kappa = 10^{[\text{Y}/\text{H}]_{\text{int}}} \left(10^{[\text{X}/\text{Y}]_{\text{int}}} - 10^{[\text{X}/\text{Y}]_{\text{gas}}} \right), \quad (7)$$

where in this case $\text{X}=\text{Fe}$ and $\text{Y}=\text{Zn}$.

Our discussion emphasizes the importance of estimating the intrinsic, nucleosynthetic ratio, $[\text{Zn}/\text{Fe}]_{\text{int}}$. On the other hand, the observed Zn abundances are not sufficiently low for the asymptotic approach to $[\text{Zn}/\text{Fe}]_{\text{int}}$ to be detected. Specifically, because the Zn II transitions are weak, only two damped Ly α systems with $[\text{Zn}/\text{H}] < -1.5$ have been detected (Lu, Sargent, & Barlow 1998; Molaro et al. 2000; Prochaska & Wolfe 2001). By contrast, clouds of such low metallicity can be easily detected in the strong Si II transitions, as shown in Figure 8b, which plots $[\text{Si}/\text{Fe}]$ versus $[\text{Si}/\text{H}]$ down to $[\text{Si}/\text{H}] = -2.6$. The figure gives convincing evidence that in the limit of vanishing metallicity, $[\text{Si}/\text{Fe}]$ approaches ≈ 0.3 rather than 0. Furthermore, at metallicities $[\text{Si}/\text{H}] > -1$ we see evidence for an increase in $[\text{Si}/\text{Fe}]$ with increasing $[\text{Si}/\text{H}]$. This is the same phenomenon seen in the $[\text{Zn}/\text{Fe}]$ versus $[\text{Zn}/\text{H}]$ diagram, which we plausibly attributed to dust. The amplitude of the increase is weaker for $[\text{Si}/\text{Fe}]$ because Si is weakly depleted. On the other hand the increase of $[\text{Si}/\text{Fe}]$ with $[\text{Si}/\text{H}]$ is stronger evidence for dust since the nucleosynthetic origin of Si is better understood than that of Zn (Hoffman et al. 1996).

3.3.2 Nucleosynthetic Abundance Patterns

• α Enhancements?

In § 3.3.1 we argued that the asymptotic behavior exhibited by the $[\text{Si}/\text{Fe}]$ ratio in the limit $[\text{Si}/\text{H}] \ll 0$ (Figure 8b) indicated a nucleosynthetic ratio, $[\text{Si}/\text{Fe}]_{\text{int}} \approx 0.3$. This asymptotic limit is robust, as it is based on a large number (56) of precision measurements obtained with echelle spectrometers on 8- to 10-m class telescopes. It also has important implications for the chemical evolution of damped Ly α systems if it equals the intrinsic nucleosynthetic ratio. The reason is that disk stars in the Galaxy exhibit a systematic decrease of $[\alpha/\text{Fe}]$ with increasing $[\text{Fe}/\text{H}]$, which indicates the increase with time of Fe contributed to the Galaxy ISM by type Ia supernovae relative to type II supernovae (Edvardsson et al. 1993). The presence of such trends in damped Ly α systems would support the argument that they are the progenitors of ordinary galaxies. However, the existence of intrinsic α enhancements in damped Ly α systems is controversial. Using the Vladilo (1998, 2002a) models, Vladilo (2002b) and Ledoux, Bergeron, & Petitjean (2002) examined $[\text{Si}/\text{Fe}]$ ratios corrected for depletion effects and found median values of $[\text{Si}/\text{Fe}]_{\text{int}}$ consistent with solar. Similarly, several studies of the depletion-free $[\text{O}/\text{Zn}]$ and $[\text{S}/\text{Zn}]$ ratios resulted in $[\alpha/\text{Zn}]$ ratios below

those of metal-poor stars (Molaro et al. 2000; Centuri3n et al. 2000; Nissen et al. 2004).

Is it possible to resolve these conflicts? The lower values of $[\alpha/\text{Zn}]$ are compatible with the higher value of $[\alpha/\text{Fe}]_{\text{int}}$ indicated by Figure 8b since $[\alpha/\text{Fe}] = [\alpha/\text{Zn}] + [\text{Zn}/\text{Fe}]$ and Prochaska et al. (2000) and Chen, Kennicutt, & Rauch (2005) find $[\text{Zn}/\text{Fe}] \approx 0.15$ for thick disk stars with $-0.9 < [\text{Fe}/\text{H}] < -0.6$, while Nissen et al. (2004) find $[\text{Zn}/\text{Fe}] \approx 0.1$ for stars with $[\text{Fe}/\text{H}] < -1.8$. Both results are consistent with $[\text{Si}/\text{Fe}]_{\text{int}} \approx 0.2$ to 0.4 . If such α enhancements are confirmed in damped Ly α systems, one would conclude that the depletion corrections used by Vladilo (2002a) and Ledoux, Bergeron, & Petitjean (2002) were too large. The latter are compatible with the dust content suggested by the Pei, Fall, & Bechtold (1991) study of reddening in damped Ly α systems. But, since the more recent study of Murphy & Liske (2004) argues against such a high dust content, the depletions used to correct the $[\text{Si}/\text{Fe}]$ ratios may be too large. We also note that $[\alpha/\text{Fe}]_{\text{int}} = 0$ would imply significant depletion of Fe at $[\text{Si}/\text{H}] < -1$, which is apparently at odds with the insensitivity of $[\text{Si}/\text{Fe}]$ to increases in $[\text{Si}/\text{H}]$ shown in Figure 8b. But this behavior may result from two compensating effects: an increase in $[\text{Si}/\text{Fe}]$ due to Fe depletion and a decrease in $[\text{Si}/\text{Fe}]$ due to increasing Fe enrichment from type Ia supernovae. Because of these uncertainties, it may be premature to use the $[\alpha/\text{Fe}]$ ratios in damped Ly α systems as discriminants between competing galaxy formation scenarios (e.g. Tolstoy et al. 2003; Venn et al. 2004).

- *Nitrogen Enrichment*

Pettini, Lipman, & Hunstead (1995) first detected nitrogen in damped Ly α systems and suggested the $[\text{N}/\alpha]$ versus $[\alpha/\text{H}]$ plane could be used as a clock to infer their ages. According to Henry, Edmunds, & K3ppen (2000) a burst of star formation would coincide with the injection of α elements into the surrounding ISM by type II supernovae, followed by the injection of ^{14}N by AGB stars more than 0.25 Gyr later. In the local Universe, one identifies a plateau of $[\text{N}/\alpha]$ values (with value ≈ -0.7 dex) at low metallicity presumably consisting of objects with ages greater than 0.25 Gyr. Within this interpretation, metal-poor objects with ages less than 0.25 Gyr would have systematically lower $[\text{N}/\alpha]$ values while more evolved damped Ly α systems, in which ^{14}N production has caught up, would have $[\text{N}/\alpha] \approx -0.7$. Recent studies (Prochaska et al. 2002a; Pettini et al. 2002; Centuri3n et al. 2003) have shown that the majority of $[\text{N}/\alpha]$ values for the damped Ly α systems are near the plateau but there is a population of damped Ly α systems with $[\text{N}/\alpha] \approx -1.5$ and very few damped Ly α systems with intermediate $[\text{N}/\alpha]$ values. The damped Ly α systems with $[\text{N}/\alpha] = -0.7$ must be older than 0.25 Gyr, indicating they are not transient objects as suggested in some schemes (see Qian & Wasserburg 2003) but rather have ages comparable to the age of the Universe at $z \sim 3$.

The observations also pose a challenge to interpreting the $[\text{N}/\alpha]$ value as a strict age diagnostic. If the ages of the damped Ly α systems are comparable to 2.5 Gyr, the age of the Universe at $z \approx 2.5$, then fewer than 10% of the objects would have $[\text{N}/\alpha] = -1.5$, contrary to current observation. Prochaska et al. (2002a) interpret the paucity of systems with $-1.5 < [\text{N}/\alpha] < -0.7$ as evidence for a bimodal IMF where systems near the plateau at $[\text{N}/\alpha] = -1.5$ are drawn from an IMF truncated from below at $M = 7.5 M_{\odot}$. In this scenario, damped Ly α systems near the plateau at $[\text{N}/\alpha] = -1.5$ need not be younger than 0.25 Gyr, while systems near the plateau at $[\text{N}/\alpha] = -0.7$ are objects older than 0.25

Gyr in which N production is due to the full mass range of intermediate-mass stars drawn from a standard IMF. More recently Molaro (2003) argued against a bimodal IMF by suggesting that damped Ly α systems near the $[N/\alpha]=-1.5$ plateau are younger than the 0.25 Gyr “catch-up” time. Meynet & Maeder (2002) and Chiappini, Matteucci, & Meynet (2003) suggested a mechanism for obtaining a more uniform distribution between the two plateaus. They showed that stellar rotation causes enhanced mixing between the H-burning and He-burning layers, thereby producing greatly enhanced ^{14}N production in massive stars. Meynet & Maeder (2002) reproduced the $[N/\alpha]=-1.5$ plateau for stars with $M=8\text{--}120 M_{\odot}$ for rotation speeds $v\sin i=400 \text{ km s}^{-1}$. Moreover, rotation may extend the effective lag time between N and α production for intermediate mass stars beyond 0.25 Gyr. However, the lack of many damped Ly α systems with $[N/\alpha]$ in between -1.5 and -0.7 dex argues against this mechanism and in favor of the bimodal IMF.

- *Metal-Strong damped Ly α system*

There exists a small subset of damped Ly α systems for which the product of HI column density and metallicity imply very strong metal-line transitions. These ‘metal-strong’ damped Ly α systems yield abundance measurements for over 20 elements including O, B, Ge, Cu, and Sn. Figure 9 shows the elemental abundance pattern obtained for DLA0812+32, the $z = 2.626$, metal-rich damped Ly α system discussed in § 3.1 (Prochaska, Howk, & Wolfe 2003c). This is the first damped Ly α system for which absolute abundances for B and Ge have been determined, and it is one of the few objects for which an accurate measurement of $[O/H]$ is possible. With the detection of over 20 elements, the metal-strong damped Ly α systems permit a global inspection of its enrichment history. The dotted line in Figure 9 is the solar abundance pattern scaled to oxygen. The good match to the data shows that this system exhibits an enrichment pattern resembling that of the Sun. Furthermore, specific abundance ratios constrain various nucleosynthetic processes in the young Universe. For example, the abundance of the odd- Z elements P, Ga, and Mn compared to Si, Ge, and Fe, indicates an enhanced “odd-even effect” and impact theories of explosive nucleosynthesis. Similarly, measurements of the B/O ratio help develop theories of light element nucleosynthesis while constraints on Sn, Kr, and other heavy elements will test scenarios of the r and s-process.

4 IONIZED GAS

The best evidence for ionized gas in damped Ly α systems comes from the detection of C IV $\lambda\lambda$ 1548.1, 1550.7 in every object for which accurate spectra have been obtained. Examples of the C IV velocity profiles are shown in Wolfe & Prochaska (2000a) who compare them with the corresponding low-ion profiles. The absence of a one-to-one alignment between the velocity components indicates that the gas producing C IV absorption is not the same gas that produces low-ion absorption. The difference is not surprising. While the X-ray background at $z \sim 3$ is about 30 times brighter than at $z = 0$ (Haardt & Madau 2003), it is still not sufficiently bright to produce C^{3+} ions by photoionization in neutral gas with Lyman limit optical depths, $\tau_{LL} >> 10^3$ (Wolfe et al. 2004). Note, collisional ionization is ruled out, as many of the C IV profiles exhibit components with $\sigma_v < 5 \text{ km s}^{-1}$ indicating $T < 3 \times 10^4 \text{ K}$, which is lower than the $T > 4 \times 10^4 \text{ K}$ threshold

required to produce significant fractions of C^{3+} . In that respect damped Ly α systems differ from the ISM in which (a) C^{3+} is collisionally ionized in gas with $T \sim 10^5$ K (Sembach & Savage 1992), and (b) the velocity components of the C IV and low- ions are aligned. This is interpreted as evidence for corotation of hot halo gas with the neutral disk (Savage, Edgar, & DiPlas 1990). By contrast, the C^{3+} ions in damped Ly α systems are more likely produced in gas that is photoionized, has a temperature $T \sim 10^4$ K, and is kinematically distinct from the neutral gas.

Damped Ly α systems also exhibit Si IV $\lambda\lambda 1393.7, 1402.7$ and Al III $\lambda\lambda 1854.7, 1862.7$ absorption. Because the Si IV and C IV velocity components are closely aligned, the Si^{+3} ions must be produced by photoionization in the same gas containing the C^{3+} ions (Wolfe & Prochaska 2000a). In the ISM the Al III lines arise in a warm ionized medium (WIM), which is an extensive region of warm ($T \sim 10^4$ K) photoionized hydrogen that pervades the disk of the Galaxy (Reynolds 2004). Therefore, it is surprising that in damped Ly α systems the Al III velocity components are aligned with the low ions and misaligned with the C IV and Si IV components which arise in gas resembling a WIM. This implies that the Al^{2+} and low ions both arise either in neutral gas or they arise in photoionized gas, which is kinematically distinct from the C^{3+} bearing gas. Photoionization equilibrium calculations indicate that in most damped Ly α systems both Al^{2+} and the low ions arise in gas that is mainly neutral (Vladilo et al. 2000; Prochaska et al. 2002b; Wolfe et al. 2004). The soft X-ray background at $z \sim 3$ is sufficiently bright to produce Al^{2+} by photoionization and to leave hydrogen mainly neutral and carbon singly ionized (see Wolfe et al. 2004). On the other hand in about 10 % of damped Ly α systems the regions giving rise to low ion and Al III absorption contain hydrogen that is significantly ionized. These cases can be recognized by the large Fe^{2+}/Fe^+ ratios and low Ar^0/Si^+ ratios (Prochaska et al. 2002b).

These studies raise some interesting questions. First, photoionization by X-ray background radiation produces ions X^j for which the ionization potential of the preceding ionization state $IP(X^{j-1}) > 1$ Ryd. In many damped Ly α systems photoionization by locally generated radiation with $h\nu < 1$ Ryd produces low ions for which $IP(X^{j-1}) < 1$ Ryd (see § 8). The question is why doesn't local radiation with $h\nu \geq 1$ Ryd photoionize sufficient neutral gas to generate a co-rotating WIM like that in the Galaxy? The answer may be related to the higher neutral gas content of damped Ly α systems, which could reduce the escape fraction of ionizing radiation from H II regions in damped Ly α systems. Second, do damped Ly α systems contain hot ($T > 10^5$ K) collisionally ionized gas? Hot gas is a byproduct of feedback processes such as galactic winds or shock heating by supernova remnants (Ferrara & Salvaterra 2004). Because of the evidence for type II supernovae (see § 3.3.2) and the possible existence of winds (see § 2.5.2), hot gas could be present in damped Ly α systems. The most efficient technique for finding hot gas is through the detection of the O VI $\lambda\lambda 1031.9, 1037.6$ doublet (Sembach et al. 2003). But no surveys for O VI in damped Ly α systems have been carried out.

5 MOLECULAR GAS

Molecular gas is ubiquitous throughout the Galaxy ISM. In a survey for Lyman and Werner band absorption, the most efficient tracers of H_2 molecules in diffuse

interstellar gas, Savage et al. (1977) detected H_2 in 90 out of 103 sightlines toward background Galactic stars. More specifically, Savage et al. (1977) showed that the molecular fraction, $f(\text{H}_2) \equiv 2N(\text{H}_2)/[2N(\text{H}_2)+N(\text{H I})]$, undergoes a steep transition from $f(\text{H}_2) < 10^{-4}$ at $N(\text{H I}) < 4 \times 10^{20} \text{ cm}^{-2}$ to $f(\text{H}_2) \geq 10^{-2}$ at $N(\text{H I}) > 4 \times 10^{20} \text{ cm}^{-2}$. Because of the similarity with the $N(\text{H I}) \geq 2 \times 10^{20} \text{ cm}^{-2}$ threshold, one might expect to find $f(\text{H}_2) > 10^{-2}$ in a significant fraction of damped $\text{Ly}\alpha$ systems. Furthermore, if damped $\text{Ly}\alpha$ systems are the neutral gas reservoirs for star formation at high redshifts, and since stars form out of molecular clouds, molecules should be present.

However, the H_2 content of damped $\text{Ly}\alpha$ systems is much lower than in the Galaxy. In their compilation of accurate searches for H_2 , Ledoux, Petitjean, & Srianand (2003) report the detection of H_2 in only five out of 23 cases qualifying as confirmed damped $\text{Ly}\alpha$ systems, which brings to mind the H_2 content of the LMC and SMC. In particular Tumlinson et al. (2002) found H_2 in only 50% of the sightlines through the LMC. Moreover, the LMC resembles the damped $\text{Ly}\alpha$ systems in that the typical upper limits are $f(\text{H}_2) < 10^{-5}$. In addition, the mean value of $f(\text{H}_2)$ for the positive detections is about 10^{-2} for the damped $\text{Ly}\alpha$ systems, the LMC and the SMC, which is about a factor of 10 lower than in the Galaxy.

Why is the H_2 content in damped $\text{Ly}\alpha$ systems so low? The answer is partially related to low dust content. In the ISM, H_2 forms on the surfaces of dust grains and is destroyed by photodissociation due to FUV radiation. In that case $f(\text{H}_2) = 2Rn_{\text{H}}/I$ (Jura 1974), where R is the formation rate constant and I is the photodissociation rate. Because $R \propto \kappa n_{\text{H}}^2$, $f(\text{H}_2)$ is predicted to decrease with decreasing dust-to-gas ratio, and since $I \propto J_{\nu}$, where J_{ν} is the mean intensity of FUV radiation, $f(\text{H}_2)$ should decrease with *increasing* radiation intensity. The low molecular fractions of the LMC and SMC are plausibly attributed to low dust content and high radiation intensities. Similarly, the low dust content of damped $\text{Ly}\alpha$ systems helps to explain the low values of $f(\text{H}_2)$. Indeed Ledoux, Bergeron, & Petitjean (2002) find a statistically significant positive correlation between $f(\text{H}_2)$ and κ .

What is the value of J_{ν} in damped $\text{Ly}\alpha$ systems? Levshakov et al. (2002) inferred J_{ν} for DLA0347–38 at $z = 3.025$ by showing that FUV pumping was responsible for populating several excited rotational levels in the ground electronic state. By combining the excitation equations with the formation equations it is possible to deduce I , independent of the functional form of R , and from that, J_{ν} . Levshakov et al. (2003) found that J_{ν} was comparable to the ambient interstellar radiation intensity in the Galaxy, i.e., $J_{\nu} \approx 10^{-19} \text{ ergs cm}^{-2} \text{ s}^{-1} \text{ Hz}^{-1} \text{ sr}^{-1}$ for this system. Previous authors reached similar conclusions for other damped $\text{Ly}\alpha$ systems (see Black, Chaffee, & Foltz 1987; Petitjean, Srianand, & Ledoux 2000; Ge & Bechtold 1997). This is an important result, because intensities of this magnitude are significantly higher than the background radiation intensity predicted at $h\nu \approx 10 \text{ eV}$ and $z \approx 3$ (Haardt & Madau 2003). Therefore, a local source of radiation is required to maintain the right balance between H_2 formation and destruction.

While the molecular content of the diffuse gas detected in damped $\text{Ly}\alpha$ systems is low, dense molecular clouds with high dust content could be present. Such objects would be missed owing to obscuration of the background QSOs or due to a low covering factor. While future surveys for radio-selected damped $\text{Ly}\alpha$ systems may eventually rule out such scenarios, they are consistent with the

current data. In fact dense molecular clouds may be required as the sites of the star formation which has been inferred for damped Ly α systems.

6 KINEMATICS

As described in the previous sections, the introduction of echelle spectrometers on 8 to 10 m-class telescopes has led to precise column density measurements of weak transitions in the damped Ly α systems. It has also led to another significant advance in damped Ly α research, namely the resolution of kinematic characteristics from the velocity profiles of the metal lines. In § 3.1 we showed that damped Ly α profiles exhibit multiple components that are qualitatively similar to the component structure of similar transitions observed in the Galaxy ISM (e.g. Wolfe et al. 1994). At high signal-to-noise ratios the line-profiles generally decompose into 5 to 30 velocity components, i.e., ‘clouds’, with column densities spanning roughly an order of magnitude. The velocity components comprising the low-ion profiles (e.g. Si II λ 1808.0) are typically broadened by turbulent motions and have velocity dispersions of $\sigma_v \approx 4\text{--}7 \text{ km s}^{-1}$. These characteristics are also observed for the high-ion profiles (e.g. C IV λ 1548.1; Wolfe & Prochaska 2000a), although the velocity dispersions are generally larger.

Prochaska & Wolfe (1997) presented the first modest sample of measurements on the low-ion kinematic characteristics of the damped Ly α systems. Their results and subsequent surveys have shown that the damped Ly α systems exhibit velocity widths Δv ranging from 15 km s^{-1} to several hundred km s^{-1} with a median of $\approx 90 \text{ km s}^{-1}$ (Figure 10). Prochaska & Wolfe (1997, 1998) demonstrated that the observed Δv distribution matched that predicted for rotating disks with typical velocity speed $v_c \sim 200 \text{ km s}^{-1}$ under the important assumption that the gas disk is thick ($h > 0.1R_d$), where h is the disk scale height and R_d is the radial exponential scale length. The authors also stressed that the damped Ly α line-profiles tend to show the ‘edge-leading asymmetry’ expected for rotating disks. The observations, therefore, suggested a population of disk galaxies with rotation speeds corresponding to present-day galaxies.

The difficulty with this scenario, however, is that hierarchical cosmology implies that galaxies in the young Universe have smaller masses and lower rotation speeds (on average) than the current population. Indeed, Prochaska & Wolfe (1997) emphasized that the circular velocity distribution of damped Ly α systems predicted within the CDM cosmogony (Kauffmann 1996) is incompatible with the observations. This includes models (e.g. Mo, Mao, & White 1998) which allow for a cross-section weighted distribution of spin parameters (Wolfe & Prochaska 2000a). As emphasized by Jedamzik & Prochaska (1998) and Prochaska & Wolfe (2001), there is a tension within CDM theory between including enough low mass galactic halos to match the observed incidence of damped Ly α systems without severely underpredicting the Δv distribution. Granted the many successes of CDM theory, perhaps it will remain a true coincidence that the damped Ly α kinematic characteristics are best described by a population of galaxies similar to (albeit thicker than) the present-day disk population.

If we are to adopt the Λ CDM power spectrum at $z \sim 3$, then the velocity fields of a significant fraction of damped Ly α systems must have contributions from non-rotational dynamics in order to explain the kinematic data. Numerical simulations within the CDM context describe the damped Ly α systems as mul-

tiple ‘proto-galactic clumps’ bound to a virialized dark matter halo (Haehnelt, Steinmetz, & Rauch 1998). The kinematics within this scenario are due to the combination of infall, random motions, and rotational dynamics. In order for this model to be consistent with the observations, however, one requires that the damped Ly α cross-section A is proportional to v_c^α with $\alpha > 2$ (Haehnelt, Steinmetz, & Rauch 1998; Maller et al. 2001). As discussed in § 2.5.2, early numerical work indicated $A \propto v_c^{1.1}$ which implied a crisis between theory and observation (Prochaska & Wolfe 2001). More recent results, however, support $A \propto v_c^{2.5}$ (Nagamine, Springel, & Hernquist 2004a) and the protogalactic clump scenario remains a viable option⁵. We stress, however, that no cosmological simulation to date has self-consistently matched the low-ion damped Ly α kinematic observations.

Lu et al. (1996) first remarked that the high-ion profiles (e.g. C IV λ 1548.1) of the damped Ly α systems have significantly different kinematic characteristics from the low-ion gas. Wolfe & Prochaska (2000a) examined a large sample of high-ion damped Ly α profiles and stressed that while the component structure is generally disjoint from the low-ion profiles, the high-ions are roughly centered on the low-ion transitions. Furthermore, there is a connection between the velocity fields of the two ionization states in that the high-ion gas nearly always shows comparable or larger velocity width than the low-ion gas (Figure 11). These trends place important constraints on the nature of the damped Ly α systems. Wolfe & Prochaska (2000b) considered a simple model where the low-ion gas is confined to a disk enshrouded in a halo of high-ion gas with kinematics described by the infall model of Mo & Miralda-Escudé (1996). Wolfe & Prochaska (2000b) demonstrated that this model could not simultaneously match the low and high-ion kinematics, in particular the co-alignment of the profile centers. In contrast, Maller et al. (2003) demonstrated that a damped Ly α model based on multiple satellites bound to a single dark matter halo can satisfy the low-ion and high-ion kinematics provided each satellite has a halo of C IV producing gas. Their model only marginally reproduced the correlation between low-ion and high-ion gas and the authors suggested that a kinematic correlation exists beyond their simple model. Perhaps numerical simulations of the hot and cold phases will show that the hot gas co-rotates with the cold gas.

Because damped Ly α systems are selected solely on the basis of H I column density, it is possible that other mechanisms contribute to their velocity fields. This could include winds induced by mergers or star formation (Nulsen, Barcons, & Fabian 1998; Schaye 2001) or even Hubble flow motions in the ambient IGM. At present such scenarios have not been quantitatively developed or tested against observation.

One can gain further insight into the nature of damped Ly α systems by synthesizing the results on kinematic characteristics with their other properties. Wolfe & Prochaska (1998) first noted relationships between the velocity width and the H I column density and metallicity of the damped Ly α systems. They found that the damped Ly α systems with larger velocity width tend to have higher metallicity. This trend matches one’s physical intuition: If the velocity width is correlated with the galactic mass, a correlation between Δv and $[M/H]$ is natural provided more massive galaxies have higher metallicity. In contrast to the metallicity- Δv

⁵We note that in the clump model the ‘edge-leading asymmetry’ can be reproduced if 3 or fewer clumps are intercepted by the majority of damped Ly α sightlines.

distribution, the damped Ly α systems show smaller $N(\text{H I})$ at large Δv values. The observations run contrary to expectation for disk galaxies where the gradient of rotation projected along the line of sight peaks toward the center. The proto-galactic clump scenario also would predict a mild, positive correlation (e.g. Maller et al. 2001) or no correlation depending on whether H I surface density correlates with halo mass. Therefore, the damped Ly α observations are unexpected and difficult to interpret in terms of single or multiple rotating disks. Additional studies, both observational and theoretical, on correlations between the kinematics and other damped Ly α properties would place further constraints on the processes of galaxy formation in the young Universe.

It is important to consider the implications of the damped Ly α kinematic characteristics with respect to the observed relative abundance patterns (e.g. Prochaska 2003). As noted in § 3.3.2, several authors have recently argued that dust-corrected α/Fe ratios of damped Ly α systems are roughly solar and indicate star formation histories representative of dwarf or irregular galaxies instead of massive systems (e.g. Calura, Matteucci, & Vladilo 2003; Tolstoy et al. 2003). We note, however, that the velocity widths of the majority of damped Ly α systems exceed 60 km s^{-1} and cannot be attributed to the gravitational velocity field of a single dwarf galaxy. Furthermore, there is no apparent correlation between the gas-phase Si/Fe ratio and velocity width. Therefore, a contradiction exists between the observed velocity widths and the interpretation of the damped Ly α abundance patterns in terms of absorption by a single dwarf galaxy along the line of sight. Regarding the CDM clump scenarios, in which multiple dwarf galaxies are found along the line of sight, one notes that the majority of damped Ly α systems are predicted to be embedded in dark matter halos which exceed the masses of present-day dwarf galaxies (e.g. Maller et al. 2001; Nagamine, Springel, & Hernquist 2004a) and instead correspond to the progenitors of galaxies like the Milky Way (Steinmetz 2003). It would be particularly valuable to perform a simulation which traced the star formation history and resolved the galaxy kinematics within a cosmological context to examine abundance pattern correlations with gas kinematics.

7 GALAXY IDENTIFICATIONS

In this section we describe the results of searches for galaxies physically associated with damped Ly α systems.

7.1 Galaxies with $z \geq 1.6$

Because of the presence of bright, $B \sim 18.5$, background QSOs, surveys for galaxies associated with high- z damped Ly α systems are more challenging than surveys for randomly selected galaxies. To illustrate this point consider a sightline passing through an L_* galaxy⁶ at a reasonable impact parameter of 10 kpc. At $z = 3$ the galaxy will have an AB magnitude of 24.7 and impact parameter of 1.3 arcsec. Detection of the galaxy against the QSO PSF with ground based telescopes would be exceedingly difficult even under the best seeing conditions and has even proven difficult with broadband space imaging. Using the NICMOS IR camera on the HST, Colbert & Malkan (2002) surveyed 22 damped Ly α systems

⁶As defined in the $z = 3$ Lyman Break Galaxy luminosity function of Steidel et al. (1999).

and detected only one candidate counterpart down to $H_{AB} = 23.5$, implying that most damped Ly α systems are not drawn from the luminous end of the Lyman Break Galaxy luminosity function. Warren et al. (2001) probed even deeper, to $H_{AB} = 25$, and found 41 candidate counterparts near 18 high-redshift damped Ly α systems. Broadband imaging to the necessary depth is thus limited by source confusion within reasonable impact parameters.

The most widely used techniques are searches for Ly α emission lines at the absorption redshift. The advantage of this method is that the wavelength of Ly α emission is located at the bottom of the damped Ly α absorption trough, which blocks the bright light of the background QSO. As a result, background night sky emission is the only source of external noise. Using slit spectroscopy, Foltz, Chaffee, & Weymann (1986) failed to detect Ly α emission with a $3\text{-}\sigma$ upper limit of $F \sim 10^{-16}$ ergs cm $^{-2}$ s $^{-1}$ for an unresolved object. While Hunstead, Fletcher, & Pettini (1990) claimed detection of Ly α emission from a compact source coinciding with DLA0836+11 at $z = 2.466$, this feature was not confirmed in spectra acquired by Wolfe et al. (1992) and Lowenthal et al. (1995). Nor was Ly α emission detected in imaging surveys using narrow-band interference filters or Fabry-Perot interferometers. In this case the QSO light is blocked because the bandwidth of the filter is centered on the damped Ly α line but has a narrower FWHM. This technique is ideal for impact parameters large compared to the seeing radius, since an emitter located outside a slit could still be detected in the narrow band image. Smith et al. (1989), Deharveng, Bowyer, & Buat (1990) and Wolfe et al. (1992) carried out narrow-band surveys for Ly α emission. Lowenthal et al. (1995) carried out Fabry-Perot surveys. No detections to limiting fluxes of $F \approx 5 \times 10^{-17}$ ergs cm $^{-2}$ s $^{-1}$ for unresolved objects were reported. The extended Ly α emitter associated with DLA0836+11 at $z = 2.466$ claimed by Wolfe et al. (1992) is more likely to be a galaxy associated with a lower redshift Mg II absorption system (Lowenthal et al. 1995).

The failure to detect Ly α emission could result from the destruction of resonantly trapped photons by even a small amount of dust (Charlot & Fall 1991). For this reason several groups attempted to detect damped Ly α systems in H α emission since H α photons are not resonantly trapped. Bunker et al. (1999) used IR detectors on a 4 m class ground-based telescope to search for H α in five damped Ly α systems, but none were detected (see also Mannucci et al. 1998). Of course, the failure to detect H α emission might also be due to small impact parameters, since an emitting region located within the PSF of the QSO would not be detected from the ground. However, Kulkarni et al. (2000, 2001) used NICMOS to search for H α emission from two damped Ly α systems and none was found (see Table 1).

With the recent detections of Ly α emission from at least 2 out of 18 damped Ly α systems surveyed using 8-to 10-m class telescopes (Møller et al. 2002; Møller, Fynbo, & Fall 2004), it is evident that the previous null detections of Ly α were largely due to the lower sensitivity of 4-m class telescopes. The results, summarized in Table 1, indicate that two of the three known Ly α emitters, DLA0458–02 and DLA0953+47A, would not have been detected in the earlier surveys. While the sample is too small to draw general conclusions, the results are interesting for the following reasons. First, damped Ly α systems resemble randomly selected Ly α emitters by the similarity in Ly α luminosity and in the compact size of the emission regions. Second, the small impact parameters for DLA0458–02 and DLA0953+47A suggest that the H I absorbing layers are smaller than ~ 5

kpc. However, since the H I content of DLA0458–02 is known to extend over linear scales exceeding 17 kpc (Briggs et al. 1989), the sightline to the QSO must pass close to a compact star forming region, which is embedded in a much larger layer of H I. Third, no continuum emission has been detected from the same two damped Ly α systems. The $B > 27$ limit on DLA0953+47A places this damped Ly α system near the faint end of the known luminosity function of Lyman Break galaxies.

By contrast, DLA2206–19A is a luminous Lyman Break galaxy. This emitter was first located in IR images obtained with NICMOS (Warren et al. 2001). The STIS image (Møller et al. 2002) shows rest-frame FUV stellar emission extending 1 arcsec between a bright knot and the QSO sightline. Ly α emission at the redshift of the damped Ly α system was detected from the knot with spectra obtained with the VLT (Møller et al. 2002). The magnitude integrated over the object is $V = 23$ (Møller 2004, priv. comm.), which places this damped Ly α system at the bright end of the Lyman Break luminosity function.

As a result, there is little overlap between the luminosity functions of damped Ly α systems and the $R < 25.5$ spectroscopic sample of Lyman Break galaxies (see Møller et al. 2002; Schaye 2001). Efforts to detect the clustering of damped Ly α systems with neighboring Lyman Break galaxies have so far only yielded upper limits (Gawiser et al. 2001; Adelberger et al. 2003), providing further evidence that the damped Ly α systems are nearly disjoint from the $R < 25.5$ spectroscopic sample of Lyman Break Galaxies, with DLA2206–19A a clear exception. Based on the UV continua implied by the Ly α luminosities of the other 2 damped Ly α systems detected in emission, there is growing evidence that at least some damped Ly α systems overlap with the dimmer “photometric” sample of Lyman Break Galaxies at $R < 27$ seen in the Hubble Deep Fields.

7.2 Galaxies with $z < 1.6$

While the nature of the galaxies associated with damped Ly α systems at $z > 1.6$ is still unclear, at lower redshifts there should be a close resemblance to objects drawn from the population of normal galaxies if damped Ly α systems trace the star formation history of normal galaxies. However, the low metallicities inferred for most low- z damped Ly α systems (Pettini et al. 1999; Kulkarni et al. 2005) has cast doubt on this idea and has led to the suggestion that low- z damped Ly α systems are metal-poor objects such as dwarf galaxies (Calura, Matteucci, & Vladilo 2003) or low surface-brightness galaxies (Jimenez, Bowen, & Matteucci 1999). As a result, identification of galaxies associated with damped Ly α systems at $z < 1$ is of vital importance.

There are 23 damped Ly α systems known at $z < 1.6$ (as of October 2004). Thirteen of these have been identified using spectroscopic or photometric redshift techniques (Chen & Lanzetta 2003; Chen, Kennicutt, & Rauch 2005) and possible host galaxies for an additional eight systems have been found in imaging surveys (Le Brun et al. 1997; Rao et al. 2003). Chen & Lanzetta (2003) analyzed an unbiased subset of nine galaxies with redshifts and concluded that the resultant luminosity distribution was dominated by luminous galaxies with $L/L_* > 0.1$; i.e., luminous galaxies dominate the neutral gas cross-section at $z < 1$. More specifically, they used a maximum-likelihood technique to determine the dependence of H I cross section on luminosity and showed that a cross-section weighted Schechter function with typical parameters for normal galaxies provided

a good fit to the data.

On the other hand, Rao et al. (2003) analyzed a heterogeneous sample of fourteen damped Ly α system host galaxy candidates, including objects without confirmed redshifts and concluded that the neutral gas cross-section at $z < 1$ was dominated by dwarf galaxies. Since Rao et al. (2003) did not quantify their result, this conclusion is difficult to evaluate. However, comparison with the sample of Chen & Lanzetta (2003) shows a larger fraction of galaxies with lower values of L/L_* in the Rao et al. (2003) sample. In some cases these are galaxies without confirmed redshifts at small angular separations from the damped Ly α sightline. In other instances, where two or more galaxies are found to be associated with the damped Ly α system, Rao et al. (2003) chose the lowest luminosity galaxy for the analysis because it had the smallest impact parameter. However, Chen & Lanzetta (2003) argue that in these cases, an entire group of galaxies is responsible for the absorption profile, so the object with lowest impact parameter may not be the appropriate choice. Given these uncertainties and the small sizes of the samples, we conclude that the current data are consistent with the galaxies associated with low redshift damped Ly α systems being drawn from the population of normal galaxies.

8 STAR FORMATION IN DAMPED Ly α SYSTEMS

Several lines of evidence imply that damped Ly α systems experience ongoing star formation. At $z < 1.6$ the evidence is unambiguous, since more than half the sample is associated with galaxies of stars. At $z > 1.6$ the evidence is indirect because only one damped Ly α system is identified with a resolved object of galactic dimensions that emits starlight. While starlight likely ionizes the gas that gives rise to Ly α emission in two other high- z damped Ly α systems, the starlight itself has not been directly detected. The expectation is that most of the metals seen in damped Ly α systems were generated through star formation in their host systems, but the instantaneous star formation rates characterizing this important population of objects remained unknown until recently.

8.1 Direct Emission Measurements of Star Formation Rates in Damped Ly α Systems with $z > 1.6$

Table 1 summarizes results including SFRs for the three positive detections and for objects with upper limits on SFR at $z > 1.6$. Observed lower limits on $L(\text{H}\alpha)$ were converted to upper limits on SFR using the Kennicutt (1998) calibration, $\text{SFR}(\text{M}_\odot \text{yr}^{-1}) = 7.9 \times 10^{-42} L(\text{H}\alpha) (\text{ergs s}^{-1})$. Detections of Ly α emission⁷ were combined with the expression for $L(\text{H}\alpha)$ and case B radiative recombination to find lower limits of $\text{SFR}(\text{M}_\odot \text{yr}^{-1}) = 1.1 \times 10^{-42} L(\text{Ly}\alpha) (\text{ergs s}^{-1})$. The total magnitude integrated over DLA2206–19A of $V = 23$ and the very sensitive $B > 27$ limit on DLA0953+47A (A. Bunker 2004, priv. comm.) were combined with the rest-frame UV Kennicutt (1998) calibration, $\text{SFR}(\text{M}_\odot \text{yr}^{-1}) = 1.4 \times 10^{-28} L_\nu (\text{ergs s}^{-1} \text{ Hz}^{-1})$, to set a lower limit on the SFR for DLA2206–19A and a rough upper limit for DLA0953+47A assuming no dust extinction for the latter object. An estimated dust extinction correction for DLA2206–19A (Wolfe et al. 2004), suggests an

⁷Due to its extreme sensitivity to dust extinction, Ly α emission provides a lower limit to the star formation rate as long as the AGN contribution to the emission line is negligible.

upper limit on SFR of $50 \text{ M}_\odot \text{ yr}^{-1}$, which is comparable to the SFRs of the more luminous Lyman Break galaxies (Shapley et al. 2003).

8.2 Star Formation Rates from the C II* Technique

A method recently developed by Wolfe, Prochaska, & Gawiser (2003b) makes it possible to infer the star formation rate per unit area for individual damped Ly α systems. The basic method is to use measurements of the C II* 1335.7 column density to measure the [C II] 158 μm cooling rate in the neutral gas producing the damped Ly α absorption. This is possible because the C II* λ 1335.7 transition arises from the excited $^2P_{3/2}$ state in C^+ , and spontaneous photon decay of the $^2P_{3/2}$ state to the $^2P_{1/2}$ state results in [C II] 158 μm emission, which is the principal coolant of neutral gas in the Galactic ISM (Wright et al. 1991). Under the presumed condition of thermal balance, the cooling rate equals the heating rate and it is possible to calculate the star formation rate per unit area that generates the implied heating rate.

By analogy with the Galactic ISM, Wolfe, Prochaska, & Gawiser (2003b) adopt the grain photoelectric effect as the principal heating mechanism for damped Ly α systems. In that case FUV radiation ($h\nu \approx 6$ to 13.6 eV) ejects photoelectrons from grain surfaces, which heat ambient electrons through Coulomb interactions (Bakes & Tielens 1994; Weingartner & Draine 2003). The heating rate from the grain photoelectric effect is proportional to the FUV radiation intensity J_ν , which consists of a contribution from the FUV background radiation plus a local contribution from hot stars located inside the galaxy which is proportional to the instantaneous star formation rate per unit area, $\dot{\psi}_*$.

To infer $\dot{\psi}_*$ and other properties from observations, Wolfe, Prochaska, & Gawiser (2003b) deduce the [C II] 158 μm spontaneous emission rate per H atom from the observational quantity:

$$\ell_c = \frac{N(\text{C II}^*) h\nu_{ul} A_{ul}}{N(\text{H I})} \text{ergs s}^{-1} \text{H}^{-1}, \quad (8)$$

where A_{ul} is the Einstein coefficient and $h\nu_{ul}$ is the energy of the 158 μm transition. These are known quantities, and $N(\text{C II}^*)$ and $N(\text{H I})$ are measured from the absorption line spectra. The total heating rate includes inputs due to the grain photoelectric effect, X-ray photoionization, cosmic ray ionization, C I photoionization, and collisional heating. The total cooling rate includes cooling due to Ly α , grain radiative recombination, and emission by fine-structure states of O^0 , Si^+ , Fe^+ , etc. in addition to the [C II] 158 μm fine-structure emission. Radiative excitation of the C^+ fine-structure states by CMB radiation is included because it can be significant at high redshift. Wolfe et al. (2004) showed that the heating rates predicted for the Haardt & Madau (2003) backgrounds were significantly lower than the 158 μm cooling rates implied for damped Ly α systems with detected C II* λ 1335.7 absorption, requiring active star formation to explain the observed cooling rates. On the other hand, Wolfe et al. (2004) also showed that heating by background radiation alone cannot be ruled out for systems in which C II* λ 1335.7 absorption was not detected. A summary of the ℓ_c data for damped Ly α systems (and the Galaxy) is given in Figure 12. Wolfe, Prochaska, & Gawiser (2003b) argued that the heating rate in the Galaxy is much larger than in damped Ly α systems because the dust content in the Galaxy is

at least a factor of 30 higher than in damped Ly α systems, whereas $\dot{\psi}_*$ in the Galaxy is only a factor of 2 to 3 lower than in damped Ly α systems (see below).

In the case of systems with detected C II* λ 1335.7 absorption, one compares 158 μ m emission rates computed for a range of star formation rates per unit area with the empirical quantity, ℓ_c . This results in two solutions for $\dot{\psi}_*$ corresponding to thermally stable states of a two-phase medium in which warm neutral medium (WNM) gas is in pressure equilibrium with cold neutral medium (CNM) gas: the WNM solution corresponds to gas with $T \sim 8000$ K and $n \sim 0.02$ cm $^{-3}$, and the CNM solution corresponds to gas with $T \sim 100$ K and $n \sim 10$ cm $^{-3}$. In every case the WNM solution for $\dot{\psi}_*$ is a factor of ten or more higher than the CNM solution: since C II emission in the WNM is a small fraction of the total cooling rate, the total heating rate implied for an observed value of ℓ_c must be higher in the WNM than in the CNM. Owing to the low dust optical depths of damped Ly α systems the resulting $\dot{\psi}_*$ are system-wide average star formation rates rather than local values as is the case in the dusty Galactic ISM.

This method was used by Wolfe et al. (2004) to analyze a sample of 45 damped Ly α systems, 23 with measured C II* column densities and 22 for which C II* was not detected. In the redshift interval $z = [1.6, 4.5]$ the average SFR per unit area for positive detections is $\langle \dot{\psi}_* \rangle = 11.3 \times 10^{-3}$ M $_{\odot}$ yr $^{-1}$ kpc $^{-2}$ for the CNM solution and 0.21 M $_{\odot}$ yr $^{-1}$ kpc $^{-2}$ for the WNM solution; by comparison in the Galaxy $\dot{\psi}_* \approx 4 \times 10^{-3}$ M $_{\odot}$ yr $^{-1}$ kpc $^{-2}$. However, the WNM solution is unlikely to be correct, because the bolometric background intensity produced exceeds the observational limits (see Wolfe, Gawiser, & Prochaska 2003a). This conclusion is consistent with recent evidence from individual systems; Howk, Wolfe, & Prochaska (2005) showed that the low upper limit on the optical-depth ratio of Si II* λ 1264.7 to C II* λ 1335.7 in a high-redshift damped Ly α system results in an upper limit of 800 K for the temperature in the gas producing C II*, which implies that C II* absorption arises in CNM gas in this system. Furthermore, a pure WNM solution would significantly overpredict the observed rest-frame-UV luminosity from DLA2206–19A based on its measured ℓ_c , implying that C II* absorption in this damped Ly α system arises in a CNM. It is significant that the predicted value for CNM, $J_{\nu}^{\text{CII}^*} = 1.7_{-1.0}^{+2.7} \times 10^{-18}$ ergs cm $^{-2}$ s $^{-1}$ Hz $^{-1}$ sr $^{-1}$ is the largest mean intensity inferred from the entire C II* sample. This may help to explain why DLA2206–19A is one of the rare damped Ly α systems detected in emission.

On the other hand the gas detected in absorption is more likely to be a WNM for damped Ly α systems with upper limits on C II* absorption. In this case the gas could be a pure single-phase WNM heated by background radiation alone. These damped Ly α systems would then be objects without significant star formation at the absorption epochs. Or the gas could be the WNM branch of a two-phase medium in which the SFR per unit area is similar to that found for the CNM solutions (Wolfe et al. 2004). While the absence of 21 cm absorption at $z > 3$ (Kanekar & Chengalur 2003) and the large C II/C I ratios (Liszt 2002) are consistent with the WNM hypothesis, both phenomena are also naturally explained within the context of the two-phase hypothesis. Clearly, it is important to determine which of these explanations is the correct one.

8.3 Implications

The C II* technique can also be used to obtain quantities with cosmological significance. Specifically, the SFR per unit comoving volume is given by $\dot{\rho}_* = \langle \psi_*(z) \rangle (A_*/A_p)(dN/dX)(H_0/c)$, where A_* is the intrinsic cross-sectional area occupied by stars emitting FUV radiation and A_p is the projection of the intrinsic H I area, A , on the sky.⁸ In the uniform disk model, neutral gas and stars are uniformly distributed across A , yielding the values for $\dot{\rho}_*(z)$ given in Table 2, which also summarizes the systematic uncertainties discussed at length in Wolfe, Gawiser, & Prochaska (2003a).

The total mass of stars produced in damped Ly α systems as a function of redshift can be computed by integrating over the cosmic star formation history of damped Ly α systems. The mass density of stars predicted by today, including the contribution from “normal” galaxies at $z < 1.6$, is consistent with the total current density of stars in spiral and elliptical galaxies, but this does not reveal the precise population of stars produced by high-redshift damped Ly α systems. The same star formation history will also deplete the neutral gas reservoir at high redshift in about $t_* \approx 2$ Gyr; i.e., $\Omega_g(z)$ would vanish by $z \approx 2$ if star formation starts at $z \approx 5$. Instead $\Omega_g(z)$ drops by a factor of two during this time, which argues for replenishment of neutral gas at an accretion rate $\dot{\rho}_a(z) = 0.5\dot{\rho}_*(z)$.

Wolfe, Gawiser, & Prochaska (2003a) also calculated the mass density of metals produced in damped Ly α systems by using the conversion of star formation rate to metal formation rate suggested by Madau et al. (1996) and Pettini (1999), $\dot{\rho}_{metals} = (1/42)\dot{\rho}_*$. Extrapolating to the present day, including the contribution from star formation in normal galaxies at $z < 1.6$, yields a mass of metals a few times larger than that found in spiral bulges today, which seems feasible. Integrating under the DLA cosmic star formation history at $z > 2.5$ predicts a factor of 30 higher cosmic mean metallicity due to metal enrichment of neutral gas than is observed in damped Ly α systems at $z = 2.5$ (Prochaska et al. 2003a). This sort of “missing metals” problem was first identified by Pettini (1999) for Lyman Break Galaxy star formation rates compared to damped Ly α system metallicities but that problem could be solved by assuming that damped Ly α systems are not the descendants of the star-forming Lyman Break Galaxies. The damped Ly α system “missing metals” problem appears to be fundamental and may illuminate a fundamental flaw in our understanding of the relationship between metal enrichment and star formation at high redshift. The problem is a significant challenge not only to the C II* method of measuring damped Ly α star formation rates, but to most hierarchical models, which also produce too many metals (see Nagamine, Springel, & Hernquist 2004b; Somerville, Primack, & Faber 2001)⁹. Given the other successes of the method it seems likely that the problem has a physical solution.

The simplest solution would be to hypothesize that the damped Ly α systems forming stars at $z > 2.5$ are no longer damped Ly α systems at $z = 2.5$ but have used up most of their neutral gas and now have the expected metallicities; the Lyman Break galaxies are an obvious candidate for their descendants. This is inconsistent, however, with timescale of ≈ 2 Gyr to use up most of the neutral

⁸Note that A_p equals $A(N, X)$ (see eq. 1) averaged over the column-density interval $N(\text{H I}) = [N_{min}, N_{max}]$

⁹The model of Pei, Fall, & Hauser (1999) avoids this problem by invoking significant obscuration corrections and low yields.

gas implied by the observed star formation rates, which is too long. Ejecting the metals into the IGM does not solve the problem, as the IGM metallicity predicted at $z = 2.5$ would be $[M/H] = -1.5$ i.e. about a factor of 30 higher than observed in the Lyman α forest, unless the ejected gas is so hot that most metals are in an unobservable ionization state, with the possible exception of oxygen, which might be detected in O VI $\lambda\lambda 1031.9, 1037.6$. An alternative possibility is that the metals are sequestered, with the most attractive solution being a model in which damped Ly α systems represent neutral gas on the outskirts of actively star-forming “bulge” regions with the majority of the produced metals remaining in these regions rather than polluting the damped Ly α gas or general IGM (Wolfe, Gawiser, & Prochaska 2003a). This hypothesis necessitates the conclusion that metal-rich bulge regions are underrepresented (or completely unrepresented) in the HI-weighted cosmic mean metallicity measured from DLAs. That would not be surprising given that the bulges may well have used up most of their neutral gas and/or have sufficient dust content to dim background QSOs out of optically selected samples.

9 CHEMICAL EVOLUTION MODELS for DAMPED Ly α SYSTEMS

In the “global” approximation, one averages all quantities over large comoving volumes and then solves the chemical evolution equations to deduce metal production rates from the comoving SFR, $\dot{\rho}_*(z)$, which is computed by tracking changes in the neutral gas density, $\rho_g(z)$ (Lanzetta et al. 1995; Pei & Fall 1995; Malaney & Chaboyer 1996; Edmunds & Phillipps 1997). However, the factor-of-two decrease between $z \approx 4$ and $z \approx 2$ suggests that damped Ly α systems are replenished by a net inflow of neutral gas (see § 8.3).

Pei & Fall (1995) considered models with inflow and outflow and searched for self-consistent evolution of the neutral gas, metallicity, and dust. These authors calculated the effects of obscuration on quantities deduced directly from the data, such as $N(\text{H I})$, and found that significant obscuration was necessary to explain the observations. Pei & Fall (1995) fitted the available data with analytic functions for $\rho_g(z)$ that increased with z at $z < 2$ (Lanzetta, Wolfe, & Turnshek 1995) and assumed that the net accretion rate, $\dot{\rho}_a(z)$, was proportional to $\dot{\rho}_*(z)$. When more accurate measurements of $\dot{\rho}_*(z)$ (Steidel et al. 1999) and the cosmic background radiation intensity (Hauser & Dwek 2001) became available, Pei, Fall, & Hauser (1999) also included the production of background radiation by stars in damped Ly α systems (see Fall, Charlot, & Pei 1996). With these additional constraints Pei, Fall, & Hauser (1999) worked directly from the measurements of $\rho_g(z)$ and eliminated the assumption that $\dot{\rho}_a(z)$ was proportional to $\dot{\rho}_*(z)$. The newer models reproduced the more accurate metallicity measurements not available earlier, and were consistent with measurements of the background radiation intensities and $\dot{\rho}_*(z)$. However, as we discuss in § 10, these models appear to cause more obscuration than the current observational data imply. Furthermore, the values of $\dot{\rho}_*(z)$ at $z < 2$ were inferred from changes in $\rho_g(z)$ that now appear to be spurious (Rao, Turnshek, & Nestor 2004; priv. comm.).

In the “local” approximation, one computes the chemical evolution of isolated galaxies outside a cosmological setting. A star-formation history is imposed from the outset and one solves for the chemical response of stars and gas. Adopt-

ing the slow star formation history for spiral galaxies suggested by Mateucci, Molaro, & Vladilo (1997), Lindner, Fritze-v. Alvensleben, & Fricke (1999) reproduced the slow evolution of $[\text{Zn}/\text{H}]$ with z observed in damped Ly α systems. However, these authors adopted a “closed box” model and neglected spatial gradients in all physical parameters. Calura, Matteucci, & Vladilo (2003) removed these restrictions and also reproduced the slow increase of $[\text{Zn}/\text{H}]$ with decreasing redshift using star formation histories predicted for large galactic radii in spirals or for episodic bursts in dwarf irregulars. Furthermore, they used the same models to reproduce the $[\text{Si}/\text{Fe}]$ versus $[\text{Fe}/\text{H}]$ relation after correcting for depletion. Dessauges-Zavadsky et al. (2004) used these models to explain the chemical evolution of three damped Ly α systems for which abundances of a large number of elements had been obtained. Interestingly, the predicted SFRs per unit area agree with those inferred from the C II* technique. Whereas Wolfe, Gawiser, & Prochaska (2003a) found that integrating such SFRs between $z = 5$ and 3 resulted in the overproduction of metals, Dessauges-Zavadsky et al. (2004) found that the cumulative metals produced did not exceed those observed owing to the short time-scales for metal production required to explain relative abundance ratios such as $[\text{Si}/\text{Fe}]$. However, in some cases the short time scales conflict with the conservative lower limit of 0.25 Gyr on age set by the measurement of $[\text{N}/\alpha]$ near the -0.7 plateau (see § 3.3.2). Other potential problems with these models stem from the depletion corrections applied to the $[\text{Si}/\text{Fe}]$ ratio, which may be too large (see § 10).

The most promising approach to chemical evolution is the direct one, which uses cosmological hydrodynamical simulations (see Somerville, Primack, & Faber 2001 and Mathlin et al. 2001 for semi-analytic and analytic variants of this method). The simulations unite the “local” and “global” approximations with a self-consistent evolution of stars, gas, metals, and dust within a Λ CDM cosmology. While the microphysics behind star formation and metal production cannot be included in these simulations, recipes calibrated to local observations are used to track stars and metals along with dark matter particles governed by gravity and gas particles governed by gravity and hydrodynamics. As a result, processes such as accretion of neutral gas from the IGM are described physically, and star formation is treated self-consistently rather than being imposed *ad hoc*. Moreover, merging between dark-matter halos is included for the first time.

Cen & Ostriker (1999) were the first to describe the chemical evolution of damped Ly α systems with numerical simulations. Using a low-resolution Eulerian scheme, these authors were unable to resolve the dark-matter halos giving rise to damped Ly α absorption. Nevertheless, they pointed out that metallicity is a more sensitive function of overdensity, δ , than of age: metal-poor objects such as the Ly α -forest clouds formed in low density environments ($\delta \approx 1$), while more metal-rich objects such as damped Ly α systems and Lyman Break Galaxies formed in regions of higher overdensity ($\delta > 10$). Using a more accurate version of this numerical code, Cen et al. (2003) predicted the cosmic metallicity at $z \sim 3$ to be between 0.3 and 0.5 dex higher than the observed value. They solved this “missing metals problem” (see § 8.3) by using obscuration corrections that may be larger than allowed by the results of Murphy & Liske (2004). They also predicted that, independent of metallicity, the ages of typical damped Ly α systems in the redshift interval $z=[2,4]$ would be 0.8–2 Gyr, which are consistent with the presence of the upper $[\text{N}/\alpha]$ plateau. Another prediction of interest is that the median stellar mass $M_* \sim 10^9 M_\odot$, which is a factor of 10 lower than that

of Lyman Break galaxies, indicating they are different populations.

The present state-of-the-art in cosmological hydrodynamic simulations of damped Ly α systems is represented by the recent results of Nagamine, Springel, & Hernquist (2004b) who used the SPH code described in § 2.5.2 (see also Cora et al. 2003). These authors found SFRs per unit area that agree with the predictions of the C II* technique for damped Ly α systems (Wolfe, Prochaska, & Gawiser 2003b). They also predicted an overproduction of metals by $z \approx 2.5$, but in this case by a factor of 10 compared to the observed metal abundances. The difference with Cen et al. (2003) is likely related to the lower spatial resolution of the latter simulation (about $30h^{-1}$ kpc comoving), which causes the high-metallicities of compact regions to be diluted by the low metallicities of diffuse regions. One of the interesting predictions of the Nagamine, Springel, & Hernquist (2004b) simulations is that all regions in which $N(\text{H I}) \geq 2 \times 10^{20} \text{ cm}^{-2}$ exhibit star formation. Confirmation of this prediction would favor the uniform disk model over the bulge model of star formation discussed by Wolfe, Gawiser, & Prochaska (2003a). As a result, it is important to decide whether this finding is an artifact of the star formation algorithm employed by Nagamine, Springel, & Hernquist (2004b), especially since there are regions in nearby galaxies in which $N(\text{H I}) \geq 2 \times 10^{20} \text{ cm}^{-2}$, but only low star formation rates ($\sim 10^{-5} \text{ M}_{\odot} \text{ yr}^{-1} \text{ kpc}^{-2}$) are observed Ferguson et al. (1998).

10 ARE DAMPED Ly α SAMPLES BIASED BY DUST?

Surveys for damped Ly α systems have the greatest impact if they represent a fair sample of the neutral gas in the Universe, allowing a clear probe of the evolution with redshift of the neutral hydrogen content and the metallicity of neutral gas. However, it has long been a major concern that the sample of damped Ly α systems suffers from “dust bias” i.e. the absence from a magnitude-limited QSO sample of those QSOs which suffer obscuration from dusty foreground damped Ly α systems, leading to underrepresentation of dusty damped Ly α systems in the overall sample. The easiest way to probe the existence and abundance of dust in damped Ly α systems would be to find the 2175Å bump feature superimposed in absorption on background QSO spectra. While at least one strong example has been found (Junkkarinen et al. 2004), this does not appear to be the rule (Pei, Fall, & Bechtold 1991). Without such sharp features to look for and given the wide range of intrinsic QSO spectral slopes, reddening from dust in damped Ly α systems must be searched for statistically by checking if the sample of QSOs with foreground damped Ly α systems is redder on average than a “control sample” of QSOs without foreground damped Ly α systems.

10.1 *Observational estimates of reddening*

Ostriker & Heisler (1984) pointed out that optically-selected QSO samples are biased towards those QSOs with little foreground dust extinction. Fall & Pei (1989) showed that dust in damped Ly α systems did not appear to cause the famous drop in the QSO number abundance at $z > 3$. Pei, Fall, & Bechtold (1991) detected reddening from damped Ly α systems at the 4σ confidence level and inferred dust-to-gas ratios between 1/20 and 1/5 that of the Galaxy, enough to explain the lack of observed Lyman α emission from damped Ly α systems. This led to the prediction that 10%-70% of QSOs are missing from optically-selected

samples, leading to an order of magnitude uncertainty in Ω_g , $\langle Z \rangle$, and other quantities estimated from damped Ly α systems (Fall & Pei 1993). However, the dust-to-gas ratios estimated from high-resolution echelle spectroscopy of QSOs with foreground damped Ly α systems are lower than the dust-to-gas ratios predicted by Fall & Pei (1993), reducing the uncertainty in quantities such as Ω_g to factors of 2-3. Pettini et al. (1997a) combined a metallicity of 1/15 solar with a dust-to-metals ratio of 1/2 that in the Milky Way to find a typical damped Ly α system dust-to-gas ratio of 1/30 Galactic. Using an SMC reddening curve, they predicted a dust extinction of only 0.1 magnitudes at 1500Å in the spectrum of background QSOs due to damped Ly α system dust. If a nucleosynthetic floor exists in damped Ly α systems at $[\text{Si}/\text{Fe}] \simeq 0.3$ then the dust-to-gas ratios are even lower than this, closer to 1/200 Galactic in most systems. Indeed, the detection of reddening due to damped Ly α systems by Pei, Fall, & Bechtold (1991) conflicts with the recent finding by Murphy & Liske (2004) that $E(B - V) < 0.01$ magnitudes using 81 damped Ly α systems found in a homogeneous set of SDSS Data Release 2 QSOs. The resolution of the conflict is not clear at present.

10.2 Surveys of radio-selected QSOs

An insidious (but not physically motivated) possibility would be the existence of gray dust associated with the damped Ly α systems which could cause obscuration without the telltale effect of reddening. Even this effect could be overcome by using a radio-selected sample of QSOs. The reason this has not typically been done is two-fold: (1) The ability to select QSOs within a preferred redshift range makes optical color selection more efficient. (2) Conducting optical spectroscopic follow-up on a radio-selected sample of QSOs is far more time-consuming precisely because they do not have a strict optical magnitude limit; half of the total exposure time can be required by the dimmest one or two objects. Obviously, dropping those from the survey would defeat the entire purpose of radio selection. One radio-selected sample has been published: the CORALS survey of Ellison et al. (2001) found 19 intervening damped Ly α systems towards 66 $z_{em} \geq 2.2$ radio-selected QSOs from the Parkes quarter-Jansky sample (Shaver et al. 1996), yielding a marginal increase in dN/dX and Ω_g at $\langle z \rangle = 2.37$ versus optically-selected QSO samples. These results imply that at most half of damped Ly α systems are missing from optically-selected samples. For Ω_g , the radio sample yields 1.4×10^{-3} as opposed to the value of 6.7×10^{-4} found for optically selected samples at this redshift (Prochaska & Herbert-Fort 2004), but this is only a 1.5 σ difference given the small sample size.

10.3 Empirical Estimates of Damped Ly α System Obscuration

A third way to estimate the effects of dust obscuration by damped Ly α systems is to infer this from the observed chemical abundances. Taking the observed HI column densities and the dust-to-gas ratios implied by the depletion patterns of the damped Ly α systems (see Eq. 7), it is possible to estimate the extinction in the rest-frame UV of the QSO for an assumed extinction curve. Given the lack of the observed 2175Å bump feature, it appears more reasonable to assume an SMC (Prevot et al. 1984) rather than Galactic (Cardelli, Clayton, & Mathis 1989) dust extinction law. Prochaska & Wolfe (2002) used this technique (see their Figure 24; see Prochaska 2004 for an update) to correct the observed QSO magnitudes by

this inferred extinction and then to compare the implied true magnitude with the magnitude limit of the survey used to search for damped Ly α systems (which is typically shallower than the limit of the survey used to discover the QSOs). These quantities were then compared to a bootstrap prediction of how many QSOs are expected to be missing from observed samples due to extinction by foreground damped Ly α systems. The typical range of extinction corrections runs from 0 to 0.3 magnitudes, even though half of the QSOs are so much brighter than the survey limit that they could have been seen with up to 1 magnitude of extinction. This shows that damped Ly α systems which cause between 0.3 magnitudes and 1 magnitude of extinction are rare and predicts that at most 10% of QSOs are missing from the samples probed for damped Ly α systems due to a damped Ly α dust bias.

11 ARE DAMPED Ly α SAMPLES BIASED BY GRAVITATIONAL LENSING ?

On the other hand Prochaska, Herbert-Fort, & Wolfe (2005) find that biasing due to gravitational lensing could be important. They compared the full SDSS sample of damped Ly α systems with subsamples comprising the brightest 33 % of background quasars and the faintest 33 % of background quasars. While the incidence of damped Ly α systems, dN/dX was found to be insensitive to quasar magnitude, the mass density, $\Omega_g(z)$, was found to vary significantly. Specifically, the bright subsample showed systematically higher values of $\Omega_g(z)$ than the faint subsample. To explain the independence of dN/dX on quasar magnitude, the difference must lie in the incidence of systems with large $N(\text{H I})$, which is observed to be larger in the bright subsample.

Prochaska, Herbert-Fort, & Wolfe (2005) argue that gravitational magnification of the background quasars by massive halos or disks associated the foreground damped Ly α systems could account for this systematic effect, which was first detected at the 2σ level by Murphy & Liske (2004). Whereas obscuration by dust would cause $\Omega_g(z)$ to be *lower* in the bright subsample, magnification by lensing due to exponential disks is greatest for damped Ly α systems with large values of $N(\text{H I})$ (Bartelmann & Loeb 1996; Maller et al. 1997).

Consequently, the values of $\Omega_g(z)$ in Figure (5) may be 10-20 % too high, but the evolution of $\Omega_g(z)$ with z is still likely to be correct. However, the effect could have a more important effect on damped Ly α system sample with $z < 2$ (Rao & Turnshek 2000).

12 CONCLUSIONS

We end this review with the following question: What have we learned from damped Ly α systems that we did not know before? We attempt to answer this question by listing results judged to be robust. These are also summarized in Tables 3 and 2, which describe cosmological and local properties, respectively. Table 3 lists both the medians and the means in order to show the effects of the upper limits placed on various parameters. Specifically, the means only include positively detected quantities while the medians include upper limits.

(1) Most of the neutral gas in the Universe in the redshift interval $z=[0,5]$ is in damped Ly α systems. The cosmology and mean intensity of extragalactic

radiation are sufficiently well known to justify the assumption of gas neutrality for $N(\text{H I}) \geq 2 \times 10^{20} \text{ cm}^{-2}$. The close agreement between the mass per unit comoving volume of neutral gas in damped Ly α systems and visible matter in current galaxies indicates that damped Ly α systems comprise a significant neutral-gas reservoir for star formation at high redshift.

(2) The comoving density of the neutral gas, $\Omega_g(z)$, declines by a factor of two between $z \approx 3.5$ and $z \approx 2.3$. While the evolution at $0 < z < 2.3$ is more uncertain, $\Omega_g(z)$ at $z \approx 3.5$ is a factor of three higher than at $z = 0$.

(3) Damped Ly α systems are metal-poor at all redshifts (see Table 2), but exhibit a metallicity “floor”, $[\text{M}/\text{H}] \geq -2.6$ (Table 3), indicating a different enrichment history than that of the Ly α forest.

(4) The cosmic metallicity doubles every Gyr at $z > 2$, but the median $[\text{M}/\text{H}]$ is sub-solar at $z \leq 1.6$.

(5) From the large $[\text{Zn}/\text{Cr}]$ ratios and the increase of the $[\text{Zn}/\text{Fe}]$ and $[\text{Si}/\text{Fe}]$ ratios with increasing metallicity we know that damped Ly α systems exhibit evidence for depletion by dust and that the dust content is far lower than in the Galaxy.

(6) The presence of a plateau in the $[\text{N}/\alpha]$ versus $[\alpha/\text{H}]$ plane near $[\text{N}/\alpha] \approx -0.7$ indicates a minimum age of 0.25 Gyr for damped Ly α systems, which suggests they are not transient objects but instead probably have ages comparable to the Hubble time at the absorption epoch.

(7) Ionized gas in damped Ly α systems exhibits a different velocity structure than the neutral gas, unlike the agreement between the velocity structures of these two phases in the Galaxy.

(8) H_2 and other molecules are rarely present in damped Ly α systems. Studies of those systems exhibiting H_2 absorption indicate the presence of an FUV radiation field with $J_\nu \approx 10^{-19} \text{ ergs cm}^{-2} \text{ s}^{-1} \text{ Hz}^{-1} \text{ sr}^{-1}$, which resembles (a) the interstellar radiation field in the Galaxy and (b) J_ν predicted by the C II* technique.

(9) The frequency distribution of the absorption velocity intervals, Δv , has a median of 90 km s $^{-1}$. This property cannot be reproduced by single-disk CDM scenarios proposed so far, and is difficult to reproduce for sightlines passing through dwarf galaxies. Damped Ly α systems with large values of Δv exhibit a systematic absence of low values of $[\text{M}/\text{H}]$ and high values of $N(\text{H I})$.

(10) We cannot rule out the hypothesis that galaxies identified with damped Ly α systems at $z < 1.6$ are drawn from a cross-section weighted sample of normal galaxies; i.e., an inflated populations of dwarfs is not required.

(11) C II* λ 1335.7 absorption is detected in about half of randomly-selected samples of damped Ly α systems. The inferred [C II] 158 μm cooling rates indicate heating rates far in excess of those supplied by FUV background radiation, requiring a local heat source. The evidence accumulated so far suggests that the likely site of C II* absorption is CNM gas.

Next, we describe critical unsolved problems in damped Ly α research.

(I) *What is the median mass, M_{med} , of the dark-matter halos containing damped Ly α systems?* This is the critical diagnostic for discriminating among most hierarchical models, in which $M_{\text{med}} < 10^9 M_\odot$, from hierarchical models with feedback or passive evolution models, in which $M_{\text{med}} > 10^{11} M_\odot$.

(II) *Does the damped Ly α luminosity function overlap that of Lyman Break galaxies?* Partial Overlap is suggested by the luminosities of the few objects detected in emission.

(III) *What are the properties of the interstellar gas in damped Ly α systems?* These are crucial for understanding whether or not the gas in which C II* absorption is detected can support a CNM.

(IV) *Are stars forming in damped Ly α systems when they are detected?*

(V) *How are the star formation and accretion histories of damped Ly α systems related?* The C II* technique indicates that star formation depletes the neutral gas reservoir of damped Ly α systems more rapidly than indicated by the decrease of $\Omega_g(z)$ with time at $z > 2.3$. Does this require accretion of neutral gas onto damped Ly α systems at rates comparable to the star formation rates?

(VI) *What is the solution to the “missing metals” problem?* Evidence for metal-enriched gas ejected from damped Ly α systems, or for light emitted from compact “bulge” regions would help in deciding between these hypotheses.

(VII) *What is the intrinsic nucleosynthetic [Si/Fe] ratio in damped Ly α systems?* Are the intrinsic abundances of damped Ly α systems α -enhanced?

(VIII) *What is the cosmic metallicity of low- z damped Ly α systems?* Is the column-density weighted mean metallicity of low- z damped Ly α systems biased by undersampling and by obscuration?

(IX) *How can we improve numerical simulations of damped Ly α system evolution?* The next steps involve more accurate modeling of star formation and mechanical feedback.

A major goal of damped Ly α system research is to give a clear and decisive answer to the question, “What is a damped Ly α system?” Obviously this has not yet been accomplished. Rather, what we have found is that a significant fraction of damped Ly α systems are a population of H I layers exhibiting many of the complexities of the ISM of the Galaxy. They clearly play an important role in the formation of galaxies and undoubtedly interact with other structures in the high redshift Universe through a variety of feedback mechanisms. Observations of damped Ly α systems provide an amazingly rich data set that gives information about galaxy formation unavailable by other means. Specifically, observations of damped Ly α systems are the only way to study in detail the neutral gas that gave rise to galaxies at high redshifts. We hope that the interplay between new observations and improved theoretical modeling will lead to significant insights into the process of galaxy formation.

ACKNOWLEDGMENTS

This review was written while one of us (AMW) was on sabbatical leave at the Institute of Astronomy, Cambridge, and AMW wishes to thank the Institute of Astronomy for the hospitality extended to him during his visit and for the award of a Sackler fellowship. AMW is particularly grateful to Max Pettini for many valuable discussions about our favorite mutual topic. AMW and JXP also wish to thank the Kavli Institute of Theoretical Physics, Santa Barbara, for the hospitality extended to them during their attendance at the Galaxy Intergalactic Medium Interactions program. This material is based on work supported by the National Science Foundations under Grant No. AST 03-07824 awarded to AMW and JXP and Grant No. AST-0201667 awarded to EG.

DLA	z_{DLA}^a	$z_{Ly\alpha}^b$	θ_b^c arcsec	b^d kpc	$F(Line)^e$ 10^{-17} (cgs)	SFR Diagnostic ^f	SFR $M_{\odot} \text{ yr}^{-1}$	Ref ^g
0458-02	2.0395	2.0396	0.3 ± 0.3	2.5 ± 2.5	$5.4^{+0.2}_{-0.8}$	Ly α	> 1.5	1
0953+47A	3.407	3.415	< 0.5	< 3.7	0.7 ± 0.2	Ly α , C	$0.8 \rightarrow 7.0$	2
2206-19A	1.9205	1.9229	1	8.4	26 ± 3.0	C	$26 \rightarrow 50$	3
1210+17	1.8918	0.25	2.1	< 2.5	H α	< 5.0	4
1244-34	1.8590	$0.16-0.24$	$1.4-2.0$	< 0.8	H α	< 1.6	5
8 DLAs	2.095-2.615	≈ 1.5	≈ 10.0	< 9.0	H α	< 30	6

Table 1: Measurements of Emission from Damped Ly α Systems^aAbsorption redshift of DLA^bLy α emission redshift^cDisplacement angle of emitter (or candidate) from QSO^dDisplacement distance of emitter (or candidate) from QSO^eLine flux in units of $\text{ergs cm}^{-2} \text{ s}^{-1}$. First 3 entries are Ly α and second 3 are H α ^fDiagnostic for obtaining SFR: Ly α is Ly α emission, C is FUV continuum, and H α is from H α emission.^gReference: (1) Møller et al. (2004); (2) A. Bunker (2004), priv. comm; (3) Møller et al. (2002); (4) Kulkarni et al. (2001); (5) Kulkarni et al. (2000); (6) Bunker et al. (1999)

Property	Redshift Interval	
	0.0-1.6	1.6-4.5
dN/dX	0.077 ± 0.016^b
$10^3 \Omega_g(z)$	0.96 ± 0.23^a	0.92 ± 0.21^b
$\log_{10} \dot{\rho}_*(z)$	< -1.40	-0.70 ± 0.28^c
$< Z >$	-0.81 ± 0.032	-1.33 ± 0.09

Table 2: Global Properties

^a Due to large uncertainties in individual measurements, error in mean given by propagation of experimental errors.^b Because of systematic decrease in dN/dX and $\Omega_g(z)$ with time, error in mean determined by standard deviation.^c Computed by averaging over the “WD low” and other dust models discussed in Wolfe et al. (2003a) (see their Table 1), and by assuming that both DLAs with detected and undetected C II* absorption have same mean SFR per unit area. If the SFR per unit area of the non-detections were significantly lower, $\dot{\rho}_*$ would decrease by about 0.3 dex.

Property	z	N^a	\bar{x}^b	x_{med}^c	σ^d	Min ^e	Max ^f
$\log_{10} N(\text{HI})$	$z > 1.6$	199	20.83	20.60	0.33	20.30	21.70
[M/H]	$0.3 < z < 4.9$	130	-1.11	-1.48	0.55	-2.65	0.04
[Zn/Fe]	$0.7 < z < 3.3$	38	0.54	0.42	0.25	-0.01	1.05
[α /Fe]	$0.8 < z < 4.7$	70	0.42	0.38	0.18	0.03	1.00
Δv_{low}^g	$1.7 < z$	95	114.	90.	83.7	16.	430.
Δv_{high}^h	$1.7 < z$	75	209.	190.	113.4	20.	528.
$\log_{10} f(\text{H}_2)$	$2.0 < z < 3.4$	33	-2.22	< -5.93	0.82	< -6.98	-0.64
$\log_{10} \ell_c^i$	$1.7 < z < 4.2$	57	-26.57	< -26.93	0.49	< -27.69	-25.35
G_0^j	$1.7 < z < 4.5$	39	9.6	5.4	6.5	< 0.24	23
$\log_{10} \dot{\psi}_*^k$	$1.7 < z < 4.2$	40	-1.95	-2.20	0.30	< -3.55	-1.55

Table 3: DLA Individual Summary

^aNumber of DLAs in sample^bMean value. Upper limits *excluded* in computation.^cMedian value. Upper limits *included* in computation.^dSample dispersion^eMinimum value.^fMaximum value.^gLow-ion absorption velocity interval (in km s⁻¹).^hHigh-ion (C IV) absorption velocity interval (in km s⁻¹).ⁱ ℓ_c is in units of ergs s⁻¹ H⁻¹^j J_ν in units of 10⁻¹⁹ ergs cm⁻² s⁻¹ Hz⁻¹ sr⁻¹. Computed for WD low model in Wolfe et al. (2004)^kSFR per unit area for uniform disk model (in M_⊙ yr⁻¹ kpc⁻²). Computed for WD low model in Wolfe et al. (2004)

References

1. Abazajian, K. et al. 2003, *Astron. J.*, 126, 2081
2. Adelberger, K. L., Steidel, C. C., Shapley, A. E., & Pettini, M. 2003, *ApJ*, 584, 45
3. Bahcall, J. N. & Peebles, P. J. E. 1969, *Ap. J. Lett.*, 156, L7
4. Bakes, E. L. O. & Tielens, A. G. G. M. 1994, *ApJ*, 427, 822
5. Bartelmann, M. & Loeb, A. 1996, *ApJ*, 457, 529
6. Beaver, E. A., Burbidge, E. M., McIlwain, C. E., Epps, H. W., & Strittmatter, P. A. 1972, *ApJ*, 178, 95
7. Bennett, C. L., Halpern, M., Hinshaw, G., Jarosik, N., Kogut, A., Limon, M., Meyer, S. S., Page, L., Spergel, D. N., Tucker, G. S., Wollack, E., Wright, E. L., Barnes, C., Greason, M. R., Hill, R. S., Komatsu, E., Nolte, M. R., Odegard, N., Peiris, H. V., Verde, L., & Weiland, J. L. 2003, *Ap. J. Suppl.*, 148, 1
8. Bihain, G., Israelian, G., Rebolo, R., Bonifacio, P., & Molaro, P. 2004, *Astron. Astrophys.*, 423, 777
9. Black, J. H., Chaffee, F. H., & Foltz, C. B. 1987, *ApJ*, 317, 442
10. Boissier, S., Péroux, C., & Pettini, M. 2003, *MNRAS*, 338, 131
11. Bosma, A. 1981, *Astron. J.*, 86, 1825
12. Briggs, F. H., Wolfe, A. M., Liszt, H. S., Davis, M. M., & Turner, K. L. 1989, *ApJ*, 341, 650
13. Brown, R. L. & Mitchell, K. J. 1983, *ApJ*, 264, 87
14. Brown, R. L. & Roberts, M. S. 1973, *Ap. J. Lett.*, 184, L7
15. Bunker, A. J., Warren, S. J., Clements, D. L., Williger, G. M., & Hewett, P. C. 1999, *MNRAS*, 309, 875
16. Calura, F., Matteucci, F., & Vladilo, G. 2003, *MNRAS*, 340, 59
17. Cardelli, J. A., Clayton, G. C., & Mathis, J. S. 1989, *ApJ*, 345, 245
18. Carswell, R. F., Hilliard, R. L., Strittmatter, P. A., Taylor, D. J., & Weymann, R. J. 1975, *ApJ*, 196, 351
19. Cen, R. & Ostriker, J. P. 1999, *Ap. J. Lett.*, 519, L109
20. Cen, R., Ostriker, J. P., Prochaska, J. X., & Wolfe, A. M. 2003, *ApJ*, 598, 741
21. Centurión, M., Bonifacio, P., Molaro, P., & Vladilo, G. 2000, *ApJ*, 536, 540
22. Centurión, M., Molaro, P., Vladilo, G., Péroux, C., Levshakov, S. A., & D’Odorico, V. 2003, *Astron. Astrophys.*, 403, 55
23. Charlot, S. & Fall, S. M. 1991, *ApJ*, 378, 471
24. Chen, H., Kennicutt, R. C., & Rauch, M. 2005, *ApJ*, 620, 703
25. Chen, H. & Lanzetta, K. M. 2003, *ApJ*, 597, 706
26. Chiappini, C., Matteucci, F., & Meynet, G. 2003, *Astron. Astrophys.*, 410, 257
27. Colbert, J. W. & Malkan, M. A. 2002, *ApJ*, 566, 51

28. Cole, S., Norberg, P., Baugh, C. M., Frenk, C. S., Bland-Hawthorn, J., Bridges, T., Cannon, R., Colless, M., Collins, C., Couch, W., Cross, N., Dalton, G., De Propris, R., Driver, S. P., Efstathiou, G., Ellis, R. S., Glazebrook, K., Jackson, C., Lahav, O., Lewis, I., Lumsden, S., Maddox, S., Madgwick, D., Peacock, J. A., Peterson, B. A., Sutherland, W., & Taylor, K. 2001, *MNRAS*, 326, 255
29. Cora, S. A., Tissera, P. B., Lambas, D. G., & Mosconi, M. B. 2003, *MNRAS*, 343, 959
30. Deharveng, J. M., Bowyer, S., & Buat, V. 1990, *Astron. Astrophys.*, 236, 351
31. Dessauges-Zavadsky, M., Calura, F., Prochaska, J. X., D’Odorico, S., & Matteucci, F. 2004, *Astron. Astrophys.*, 416, 79
32. Dessauges-Zavadsky, M., Prochaska, J. X., & D’Odorico, S. 2002, *Astron. Astrophys.*, 391, 801
33. Dickinson, M., Papovich, C., Ferguson, H. C., & Budavári, T. 2003, *ApJ*, 587, 25
34. D’Odorico, V. & Molaro, P. 2004, *Astron. Astrophys.*, 415, 879
35. Edmunds, M. G. & Phillipps, S. 1997, *MNRAS*, 292, 733
36. Edvardsson, B., Andersen, J., Gustafsson, B., Lambert, D. L., Nissen, P. E., & Tomkin, J. 1993, *Astron. Astrophys.*, 275, 101
37. Eggen, O. J., Lynden-Bell, D., & Sandage, A. R. 1962, *ApJ*, 136, 748
38. Ellison, S. L., Yan, L., Hook, I. M., Pettini, M., Wall, J. V., & Shaver, P. 2001, *Astron. Astrophys.*, 379, 393
39. Fall, S. M., Charlot, S., & Pei, Y. C. 1996, *Ap. J. Lett.*, 464, L43
40. Fall, S. M. & Efstathiou, G. 1980, *MNRAS*, 193, 189
41. Fall, S. M. & Pei, Y. C. 1989, *ApJ*, 337, 7
42. —. 1993, *ApJ*, 402, 479
43. Fenner, Y., Prochaska, J. X., & Gibson, B. K. 2004, *ApJ*, 606, 116
44. Ferguson, A. M. N., Wyse, R. F. G., Gallagher, J., & Hunter, D. 1998, *Ap. J. Lett.*, 506, L19
45. Ferrara, A. & Salvaterra, R. 2004, ArXiv Astrophysics e-prints, astro-ph/0406554
46. Foltz, C. B., Chaffee, F. H., & Weymann, R. J. 1986, *Astron. J.*, 92, 247
47. Fukugita, M., Hogan, C. J., & Peebles, P. J. E. 1998, *ApJ*, 503, 518
48. Gardner, J. P., Katz, N., Hernquist, L., & Weinberg, D. H. 1997a, *ApJ*, 484, 31
49. —. 2001, *ApJ*, 559, 131
50. Gardner, J. P., Katz, N., Weinberg, D. H., & Hernquist, L. 1997b, *ApJ*, 486, 42
51. Gawiser, E., Wolfe, A. M., Prochaska, J. X., Lanzetta, K. M., Yahata, N., & Quirrenbach, A. 2001, *ApJ*, 562, 628
52. Ge, J. & Bechtold, J. 1997, *Ap. J. Lett.*, 477, L73
53. Giavalisco, M., Dickinson, M., Ferguson, H. C., Ravindranath, S., Kretchmer, C., Moustakas, L. A., Madau, P., Fall, S. M., Gardner, J. P., Livio, M., Papovich, C., Renzini, A., Spinrad, H., Stern, D., & Riess, A. 2004, *Ap. J. Lett.*, 600, L103
54. Haardt, F. & Madau, P. 1996, *ApJ*, 461, 20
55. —. 2003, <http://pitto.mib.infn.it/~haardt/cosmology.html>

56. Haehnelt, M. G., Steinmetz, M., & Rauch, M. 1998, *ApJ*, 495, 647
57. Hamann, F. & Ferland, G. 1999, *Ann. Rev. Astron. Astrophys.*, 37, 487
58. Hauser, M. & Dwek, E. 2001, *Ann. Rev. Astron. Astrophys.*, 39, 249
59. Henry, R. B. C., Edmunds, M. G., & Köppen, J. 2000, *ApJ*, 541, 660
60. Hoffman, R. D., Woosley, S. E., Fuller, G. M., & Meyer, B. S. 1996, *ApJ*, 460, 478
61. Howk, J. C., Wolfe, A. M., & Prochaska, J. X. 2005, *Ap. J. Lett.*, 622, 81
62. Hunstead, R. W., Fletcher, A. B., & Pettini, M. 1990, *ApJ*, 356, 23
63. Jedamzik, K. & Prochaska, J. X. 1998, *MNRAS*, 296, 430
64. Jenkins, E. B. 1987, in ASSL Vol. 134: Interstellar Processes, 533–559
65. Jenkins, E. B. 1996, *ApJ*, 471, 292
66. Jimenez, R., Bowen, D. V., & Matteucci, F. 1999, *Ap. J. Lett.*, 514, L83
67. Jura, M. 1974, *ApJ*, 191, 375
68. Kanekar, N. & Chengalur, J. N. 2003, *Astron. Astrophys.*, 399, 857
69. Katz, N., Weinberg, D. H., Hernquist, L., & Miralda-Escude, J. 1996, *Ap. J. Lett.*, 457, L57
70. Kauffmann, G. 1996, *MNRAS*, 281, 475
71. Kennicutt, R. C. 1998, *ApJ*, 498, 541
72. Klypin, A., Borgani, S., Holtzman, J., & Primack, J. 1995, *ApJ*, 444, 1
73. Kulkarni, V. P. & Fall, S. M. 2002, *ApJ*, 580, 732
74. Kulkarni, V. P., Fall, S. M., Lauroesch, J. T., York, D. G., Welty, D. E., Khare, P., & Truran, J. W. 2005, *ApJ*, 618, 68
75. Kulkarni, V. P., Hill, J. M., Schneider, G., Weymann, R. J., Storrie-Lombardi, L. J., Rieke, M. J., Thompson, R. I., & Jannuzi, B. T. 2000, *ApJ*, 536, 36
76. —. 2001, *ApJ*, 551, 37
77. Lanzetta, K. M., McMahon, R. G., Wolfe, A. M., Turnshek, D. A., Hazard, C., & Lu, L. 1991, *Ap. J. Suppl.*, 77, 1
78. Lanzetta, K. M., Wolfe, A. M., & Turnshek, D. A. 1995, *ApJ*, 440, 435
79. Le Brun, V., Bergeron, J., Boisse, P., & Deharveng, J. M. 1997, *Astron. Astrophys.*, 321, 733
80. Ledoux, C., Bergeron, J., & Petitjean, P. 2002, *Astron. Astrophys.*, 385, 802
81. Ledoux, C., Petitjean, P., & Srianand, R. 2003, *MNRAS*, 346, 209
82. Levshakov, S. A., Agafonova, I. I., D’Odorico, S., Wolfe, A. M., & Dessauges-Zavadsky, M. 2003, *ApJ*, 582, 596
83. Levshakov, S. A., Dessauges-Zavadsky, M., D’Odorico, S., & Molaro, P. 2002, *ApJ*, 565, 696
84. Lindner, U., Fritze-v. Alvensleben, U., & Fricke, K. J. 1999, *Astron. Astrophys.*, 341, 709
85. Liszt, H. 2002, *Astron. Astrophys.*, 389, 393
86. Lowenthal, J. D., Hogan, C. J., Green, R. F., Woodgate, B., Caulet, A., Brown, L., & Bechtold, J. 1995, *ApJ*, 451, 484

87. Lu, L., Sargent, W. L. W., & Barlow, T. A. 1998, *Astron. J.*, 115, 55
88. Lu, L., Sargent, W. L. W., Barlow, T. A., Churchill, C. W., & Vogt, S. S. 1996, *Ap. J. Suppl.*, 107, 475
89. Ma, C. & Bertschinger, E. 1994, *Ap. J. Lett.*, 434, L5
90. Madau, P., Ferguson, H. C., Dickinson, M. E., Giavalisco, M., Steidel, C. C., & Fruchter, A. 1996, *MNRAS*, 283, 1388
91. Malaney, R. A. & Chaboyer, B. 1996, *ApJ*, 462, 57
92. Maller, A. H., Flores, R. A., & Primack, J. R. 1997, *ApJ*, 486, 681
93. Maller, A. H., Prochaska, J. X., Somerville, R. S., & Primack, J. R. 2001, *MNRAS*, 326, 1475
94. —. 2003, *MNRAS*, 343, 268
95. Mannucci, F., Thompson, D., Beckwith, S. V. W., & Williger, G. M. 1998, *Ap. J. Lett.*, 501, L11
96. Mathlin, G. P., Baker, A. C., Churches, D. K., & Edmunds, M. G. 2001, *MNRAS*, 321, 743
97. McDonald, P. 2003, *ApJ*, 585, 34
98. Mestel, L. 1963, *MNRAS*, 126, 553
99. Meyer, D. M., Welty, D. E., & York, D. G. 1989, *Ap. J. Lett.*, 343, L37
100. Meynet, G. & Maeder, A. 2002, *Astron. Astrophys.*, 381, L25
101. Mihalas, D. 1978, *Stellar atmospheres* (2nd edition) (San Francisco, W. H. Freeman and Co., 1978.)
102. Minchin, R. F., Disney, M. J., Boyce, P. J., deBlok, W. J. G., Parkes, Q. A., et al. 2003, *MNRAS*, 346, 787
103. Mo, H. J., Mao, S., & White, S. D. M. 1998, *MNRAS*, 295, 319
104. Mo, H. J. & Miralda-Escudé, J. 1994, *Ap. J. Lett.*, 430, L25
105. —. 1996, *ApJ*, 469, 589
106. Molaro, P. 2003, *Elemental Abundances in Old Stars and Damped Lyman- α Systems*, 25th meeting of the IAU, Joint Discussion 15, 22 July 2003, Sydney, Australia, 15
107. Molaro, P., Bonifacio, P., Centurión, M., D’Odorico, S., Vladilo, G., Santin, P., & Di Marcantonio, P. 2000, *ApJ*, 541, 54
108. Møller, P., Fynbo, J. P. U., & Fall, S. M. 2004, *Astron. Astrophys.*, 422, L33
109. Møller, P., Warren, S. J., Fall, S. M., Fynbo, J. U., & Jakobsen, P. 2002, *ApJ*, 574, 51
110. Murphy, M. & Liske, J. 2004, *MNRAS*, 354, L31
111. Nagamine, K., Springel, V., & Hernquist, L. 2004a, *MNRAS*, 348, 421
112. —. 2004b, *MNRAS*, 348, 435
113. Navarro, J. F. & Steinmetz, M. 2000, *ApJ*, 538, 477
114. Nissen, P. E., Chen, Y. Q., Asplund, M., & Pettini, M. 2004, *Astron. Astrophys.*, 415, 993
115. Nulsen, P. E. J., Barcons, X., & Fabian, A. C. 1998, *MNRAS*, 301, 168

116. Ostriker, J. P. & Heisler, J. 1984, *ApJ*, 278, 1
117. Ouchi, M., Shimasaku, K., Furusawa, H., Miyazaki, M., Doi, M., Hamabe, M., Hayashino, T., Kimura, M., Kodaira, K., Komiyama, Y., Matsuda, Y., Miyazaki, S., Nakata, F., Okamura, S., Sekiguchi, M., Shioya, Y., Tamura, H., Taniguchi, Y., Yagi, M., & Yasuda, N. 2003, *ApJ*, 582, 60
118. Péroux, C., Dessauges-Zavadsky, M., D’Odorico, S., Kim, T., & McMahon, R. G. 2003a, *MNRAS*, 345, 480
119. Péroux, C., Dessauges-Zavadsky, M., Kim, T., McMahon, R. G., & D’Odorico, S. 2002, *Astrophysics and Space Science*, 281, 543
120. Péroux, C., McMahon, R. G., Storrie-Lombardi, L. J., & Irwin, M. J. 2003b, *MNRAS*, 346, 1103
121. Pei, Y. C. & Fall, S. M. 1995, *ApJ*, 454, 69
122. Pei, Y. C., Fall, S. M., & Bechtold, J. 1991, *ApJ*, 378, 6
123. Pei, Y. C., Fall, S. M., & Hauser, M. G. 1999, *ApJ*, 522, 604
124. Petitjean, P., Srianand, R., & Ledoux, C. 2000, *Astron. Astrophys.*, 364, L26
125. Pettini, M. 1999, in Chemical Evolution from Zero to High Redshift, Proc. ESO Workshop, ed. JR Walsh and MR Rosa, Berlin: Springer Verlag, 233
126. Pettini, M. 2004, in Cosmochemistry. The melting pot of the elements, 257–298
127. Pettini, M., Boksenberg, A., & Hunstead, R. W. 1990, *ApJ*, 348, 48
128. Pettini, M., Ellison, S. L., Bergeron, J., & Petitjean, P. 2002, *Astron. Astrophys.*, 391, 21
129. Pettini, M., Ellison, S. L., Steidel, C. C., & Bowen, D. V. 1999, *ApJ*, 510, 576
130. Pettini, M., King, D. L., Smith, L. J., & Hunstead, R. W. 1997a, *ApJ*, 478, 536
131. Pettini, M., Lipman, K., & Hunstead, R. W. 1995, *ApJ*, 451, 100
132. Pettini, M., Smith, L. J., Hunstead, R. W., & King, D. L. 1994, *ApJ*, 426, 79
133. Pettini, M., Smith, L. J., King, D. L., & Hunstead, R. W. 1997b, *ApJ*, 486, 665
134. Press, W. H. & Schechter, P. 1974, *ApJ*, 187, 425
135. Prevot, M. L., Lequeux, J., Prevot, L., Maurice, E., & Rocca-Volmerange, B. 1984, *Astron. Astrophys.*, 132, 389
136. Prochaska, J. X. 1999, *Ap. J. Lett.*, 511, L71
137. —. 2003, Elemental Abundances in Old Stars and Damped Lyman- α Systems, 25th meeting of the IAU, Joint Discussion 15, 22 July 2003, Sydney, Australia, 15
138. Prochaska, J. X. 2004, in Origin and Evolution of the Elements, ed A. McWilliam, M. Rauch, Cambridge, UK: Cambridge Univ. Press, 455
139. Prochaska, J. X., Gawiser, E., Wolfe, A. M., Castro, S., & Djorgovski, S. G. 2003a, *Ap. J. Lett.*, 595, L9
140. Prochaska, J. X., Gawiser, E., Wolfe, A. M., Cooke, J., & Gelino, D. 2003b, *Ap. J. Suppl.*, 147, 227
141. Prochaska, J. X., Henry, R. B. C., O’Meara, J. M., Tytler, D., Wolfe, A. M., Kirkman, D., Lubin, D., & Suzuki, N. 2002a, *Proceedings of the Astronomical Society of the Pacific*, 114, 933

142. Prochaska, J. X. & Herbert-Fort, S. 2004, *Proceedings of the Astronomical Society of the Pacific*, 116, 622
143. Prochaska, J. X., Herbert-Fort, S., & Wolfe, A. M. 2005, ArXiv Astrophysics e-prints, astro-ph/0508361
144. Prochaska, J. X., Howk, J. C., O'Meara, J. M., Tytler, D., Wolfe, A. M., Kirkman, D., Lubin, D., & Suzuki, N. 2002b, *ApJ*, 571, 693
145. Prochaska, J. X., Howk, J. C., & Wolfe, A. M. 2003c, *Nature*, 423, 57
146. Prochaska, J. X., Naumov, S. O., Carney, B. W., McWilliam, A., & Wolfe, A. M. 2000, *Astron. J.*, 120, 2513
147. Prochaska, J. X. & Wolfe, A. M. 1996, *ApJ*, 470, 403
148. —. 1997, *ApJ*, 487, 73
149. —. 1998, *ApJ*, 507, 113
150. —. 2001, *Ap. J. Lett.*, 560, L33
151. —. 2002, *ApJ*, 566, 68
152. Qian, Y.-Z. & Wasserburg, G. J. 2003, *Ap. J. Lett.*, 596, L9
153. Rao, S. M., Nestor, D. B., Turnshek, D. A., Lane, W. M., Monier, E. M., & Bergeron, J. 2003, *ApJ*, 595, 94
154. Rao, S. M., Prochaska, J. X., Howk, J. C., & Wolfe, A. M. 2005, *Astron. J.*, 129, 9
155. Rao, S. M. & Turnshek, D. A. 2000, *Ap. J. Suppl.*, 130, 1
156. Rauch, M. 1998, *Ann. Rev. Astron. Astrophys.*, 36, 267
157. Reynolds, R. J. 2004, *Advances in Space Research*, 34, 27
158. Rhoads, J. E. & Malhotra, S. 2001, *Ap. J. Lett.*, 563, L5
159. Roberts, M. S., Brown, R. L., Brundage, W. D., Rots, A. H., Haynes, M. P., & Wolfe, A. M. 1976, *Astron. J.*, 81, 293
160. Rosenberg, J. L. & Schneider, S. E. 2002, *ApJ*, 567, 247
161. Ryan-Weber, E. V., Webster, R. L., & Staveley-Smith, L. 2003, *MNRAS*, 343, 1195
162. Sargent, W. L. W., Steidel, C. C., & Boksenberg, A. 1988, *Ap. J. Suppl.*, 68, 539
163. Savage, B. D., Drake, J. F., Budich, W., & Bohlin, R. C. 1977, *ApJ*, 216, 291
164. Savage, B. D., Edgar, R. J., & Diplas, A. 1990, *ApJ*, 361, 107
165. Savage, B. D. & Sembach, K. R. 1991, *ApJ*, 379, 245
166. —. 1996, *Ann. Rev. Astron. Astrophys.*, 34, 279
167. Schaye, J. 2001, *Ap. J. Lett.*, 559, L1
168. Schaye, J., Aguirre, A., Kim, T., Theuns, T., Rauch, M., & Sargent, W. L. W. 2003, *ApJ*, 596, 768
169. Sembach, K. R. & Savage, B. D. 1992, *Ap. J. Suppl.*, 83, 147
170. Sembach, K. R., Wakker, B. P., Savage, B. D., Richter, P., Meade, M., Shull, J. M., Jenkins, E. B., Sonneborn, G., & Moos, H. W. 2003, *Ap. J. Suppl.*, 146, 165

171. Shapley, A. E., Steidel, C. C., Pettini, M., & Adelberger, K. L. 2003, *ApJ*, 588, 65
172. Shaver, P. A., Wall, J. V., Kellermann, K. I., Jackson, C. A., & Hawkins, M. R. S. 1996, *Nature*, 384, 439
173. Sheth, R. K., Mo, H. J., & Tormen, G. 2001, *MNRAS*, 323, 1
174. Simcoe, R. A., Sargent, W. L. W., & Rauch, M. 2004, *ApJ*, 606, 92
175. Smith, H. E., Cohen, R. D., Burns, J. E., Moore, D. J., & Uchida, B. A. 1989, *ApJ*, 347, 87
176. Smith, H. E., Margon, B., & Jura, M. 1979, *ApJ*, 228, 369
177. Somerville, R. S., Primack, J. R., & Faber, S. M. 2001, *MNRAS*, 320, 504
178. Steidel, C. C., Adelberger, K. L., Giavalisco, M., Dickinson, M., & Pettini, M. 1999, *ApJ*, 519, 1
179. Steidel, C. C., Adelberger, K. L., Shapley, A. E., Pettini, M., Dickinson, M., & Giavalisco, M. 2003, *ApJ*, 592, 728
180. Steidel, C. C. & Sargent, W. L. W. 1992, *Ap. J. Suppl.*, 80, 1
181. Steinmetz, M. 2003, in ASP Conf. Ser. 291: Hubble's Science Legacy: Future Optical/Ultraviolet Astronomy from Space, 237
182. Storrie-Lombardi, L. J. & Wolfe, A. M. 2000, *ApJ*, 543, 552
183. Tolstoy, E., Venn, K. A., Shetrone, M., Primas, F., Hill, V., Kaufer, A., & Szeifert, T. 2003, *Astron. J.*, 125, 707
184. Tremonti, C. A., Heckman, T. M., Kauffmann, G., Brinchman, J., Charlot, S., et al. 2004, *ApJ*, 613, 898
185. Tumlinson, J., Shull, J. M., Rachford, B. L., Browning, M. K., Snow, T. P., Fullerton, A. W., Jenkins, E. B., Savage, B. D., Crowther, P. A., Moos, H. W., Sembach, K. R., Sonneborn, G., & York, D. G. 2002, *ApJ*, 566, 857
186. Tytler, D., Kirkman, D., O'Meara, J. M., Suzuki, N., Orin, A., Lubin, D., Paschos, P., Jena, T., Lin, W., & Norman, M. L. 2004, *ApJ*, 617, 1
187. Venn, K. A., Irwin, M., Shetrone, M. D., Tout, C. A., Hill, V., & Tolstoy, E. 2004, *Astron. J.*, 128, 1177
188. Viegas, S. M. 1995, *MNRAS*, 276, 268
189. Vladilo, G. 1998, *ApJ*, 493, 583
190. —. 2002a, *ApJ*, 569, 295
191. —. 2002b, *Astron. Astrophys.*, 391, 407
192. Vladilo, G., Bonifacio, P., Centurión, M., & Molaro, P. 2000, *ApJ*, 543, 24
193. Warren, S. J., Møller, P., Fall, S. M., & Jakobsen, P. 2001, *MNRAS*, 326, 759
194. Weingartner, J. C. & Draine, B. T. 2003, *ApJ*, 589, 289
195. Wheeler, J. C., Sneden, C., & Truran, J. W. 1989, *Ann. Rev. Astron. Astrophys.*, 27, 279
196. Wolfe, A. M. 1986, Royal Society of London Philosophical Transactions Series A, 320, 503
197. Wolfe, A. M., Briggs, F. H., & Janucey, D. L. 1981, *ApJ*, 248, 460
198. Wolfe, A. M. & Davis, M. M. 1979, *Astron. J.*, 84, 699

199. Wolfe, A. M., Fan, X., Tytler, D., Vogt, S. S., Keane, M. J., & Lanzetta, K. M. 1994, *Ap. J. Lett.*, 435, L101
200. Wolfe, A. M., Gawiser, E., & Prochaska, J. X. 2003a, *ApJ*, 593, 235
201. Wolfe, A. M., Howk, J. C., Gawiser, E., Prochaska, J. X., & Lopez, S. 2004, *ApJ*, 615, 625
202. Wolfe, A. M., Lanzetta, K. M., Foltz, C. B., & Chaffee, F. H. 1995, *ApJ*, 454, 698
203. Wolfe, A. M., Lanzetta, K. M., Turnshek, D. A., & Oke, J. B. 1992, *ApJ*, 385, 151
204. Wolfe, A. M. & Prochaska, J. X. 1998, *Ap. J. Lett.*, 494, L15
205. —. 2000a, *ApJ*, 545, 591
206. —. 2000b, *ApJ*, 545, 603
207. Wolfe, A. M., Prochaska, J. X., & Gawiser, E. 2003b, *ApJ*, 593, 215
208. Wolfe, A. M., Turnshek, D. A., Smith, H. E., & Cohen, R. D. 1986, *Ap. J. Suppl.*, 61, 249
209. Wolfire, M. G., McKee, C. F., Hollenbach, D., & Tielens, A. G. G. M. 2003, *ApJ*, 587, 278
210. Wright, A. E., Morton, D. C., Peterson, B. A., & Jauncey, D. L. 1979, *MNRAS*, 189, 611
211. Wright, E. L., Mather, J. C., Bennett, C. L., Cheng, E. S., Shafer, R. A., Fixsen, D. J., Eplee, R. E., Isaacman, R. B., Read, S. M., Boggess, N. W., Gulkis, S., Hauser, M. G., Janssen, M., Kelsall, T., Lubin, P. M., Meyer, S. S., Moseley, S. H., Murdock, T. L., Silverberg, R. F., Smoot, G. F., Weiss, R., & Wilkinson, D. T. 1991, *ApJ*, 381, 200
212. Zwaan, M. A., Briggs, F. H., & Sprayberry, D. 2001, *MNRAS*, 327, 1249

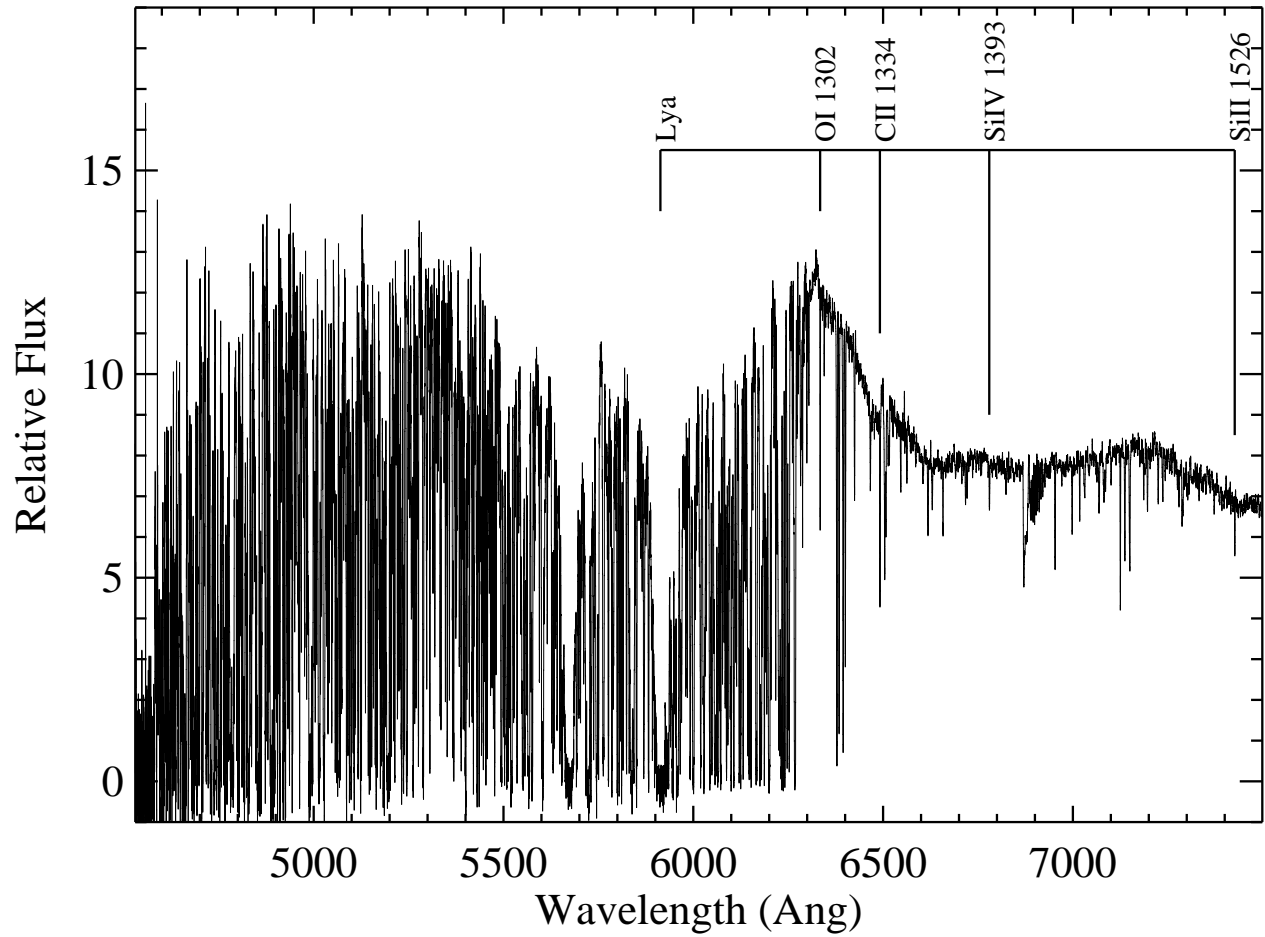


Figure 1: Keck/ESI spectrum of QSO PSS0209+0517 showing the $\text{Ly}\alpha$ forest, a pair of damped $\text{Ly}\alpha$ systems, and a series of metal-lines. The schematic labeling in the figure identifies several key features for the damped $\text{Ly}\alpha$ system at $z = 3.864$. The absorption trough at $\lambda = 5674 \text{ \AA}$ corresponds to the damped $\text{Ly}\alpha$ line at $z = 3.667$.

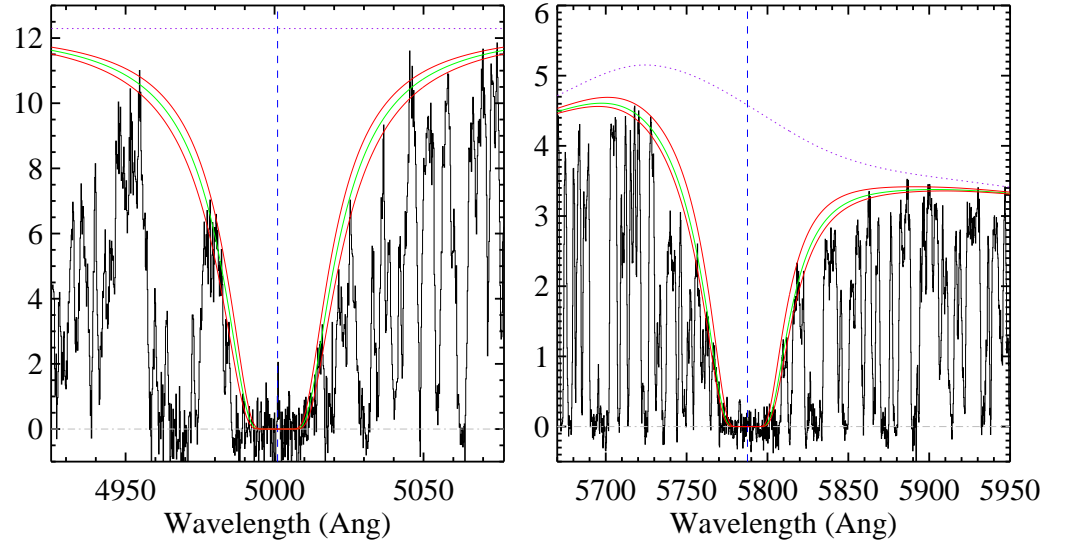


Figure 2: Example Voigt profile fits to two damped $\text{Ly}\alpha$ systems of the sample from Prochaska et al. (2003b). The vertical dashed line indicates the line centroid determined from metal-line transitions identified outside the $\text{Ly}\alpha$ forest. The dotted line traces the continuum of the QSO and the green and red lines trace the Voigt profile solution and the fits corresponding to 1σ changes to $N(\text{HI})$. The fluctuations at the bottom of the damped $\text{Ly}\alpha$ absorption troughs indicate the level of sky noise.

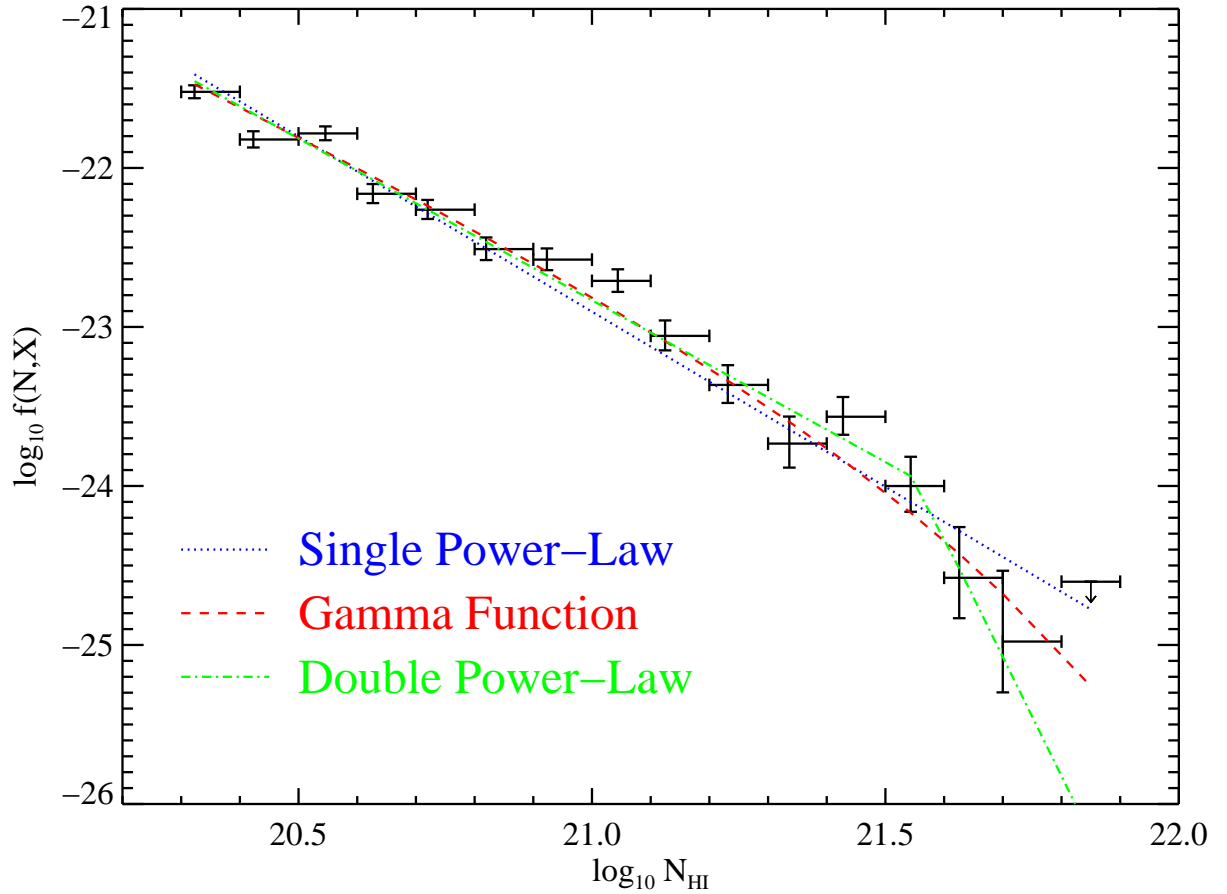


Figure 3: The $N(\text{H I})$ frequency distribution $f(N, X)$ determined by Prochaska et al. (2005) for all damped $\text{Ly}\alpha$ systems in the SDSS DR3-DR4 sample. Overplotted on the data pointst are a single power-law, Γ function, and a double power-law. On the latter two are acceptable fits to the data. Plot taken from Prochaska et al. (2005).

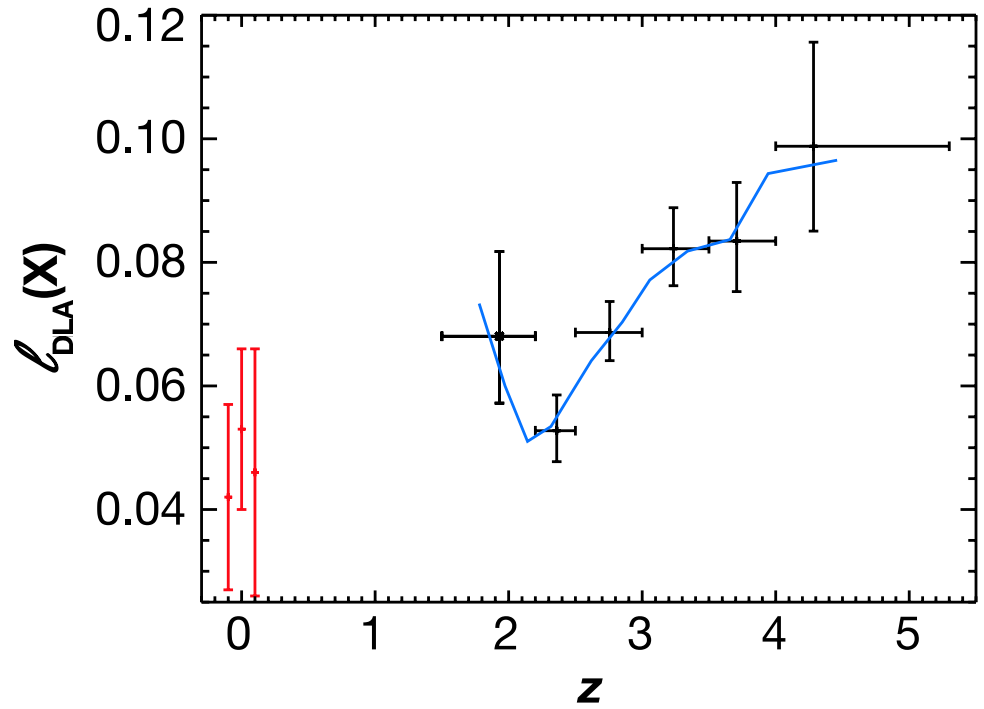


Figure 4: Incidence of damped Ly α systems per unit cosmological distance dN/dX (denote by ℓ_{DLA} in the figure) as a function of redshift. The three data points at $z = 0$ are all local measurements from 21 cm observations (Ryan-Weber, Webster, & Staveley-Smith 2003; Zwaan et al. 2001; Rosenberg & Schneider 2002). The curve overplotted on the data traces the evaluation of dN/dX in a series of 0.5 Gyr intervals. Plot taken from Prochaska et al. (2005).

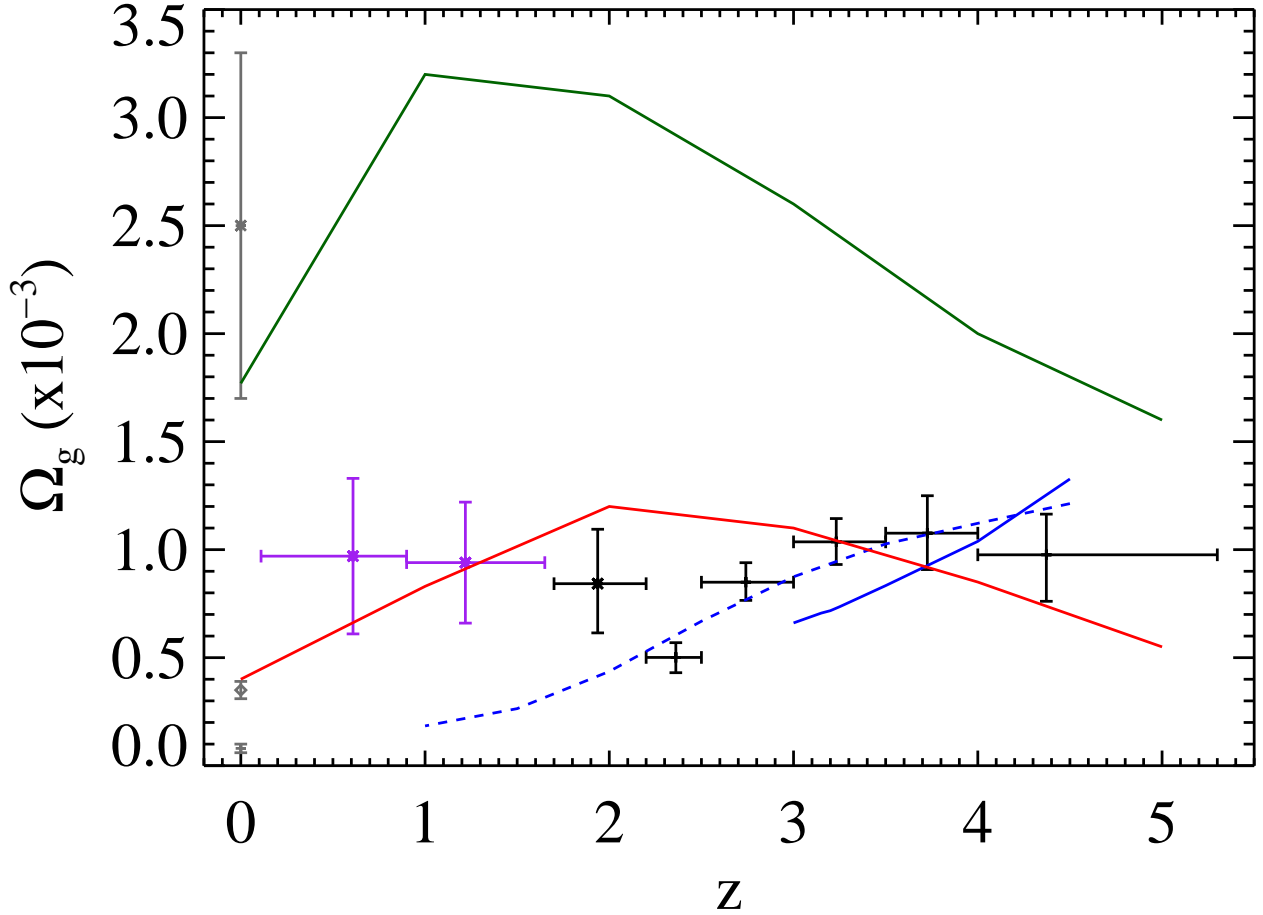


Figure 5: Neutral gas mass density versus z from Prochaska et al. (2005). H I data at (a) $z > 2.2$ from SDSS DR3-4 survey, (b) $0 < z < 1.6$ from the Mg II survey of Rao, Turnshek, & Nestor (2004, priv. comm.), and (c) at $z = 0$ (diamond) from Fukugita et al. (1998). Stellar mass density at $z = 0$ (star) from Cole et al. (2001) and stellar mass density of Irr galaxies (+ sign) from Fukugita et al. (1998). Theoretical curves from Cen et al. (2003) (*green*), Somerville et al. (2001) (*red*), and Nagamine et al. (2004a) (*blue:dotted* is D5 model and *solid* is Q5 model)

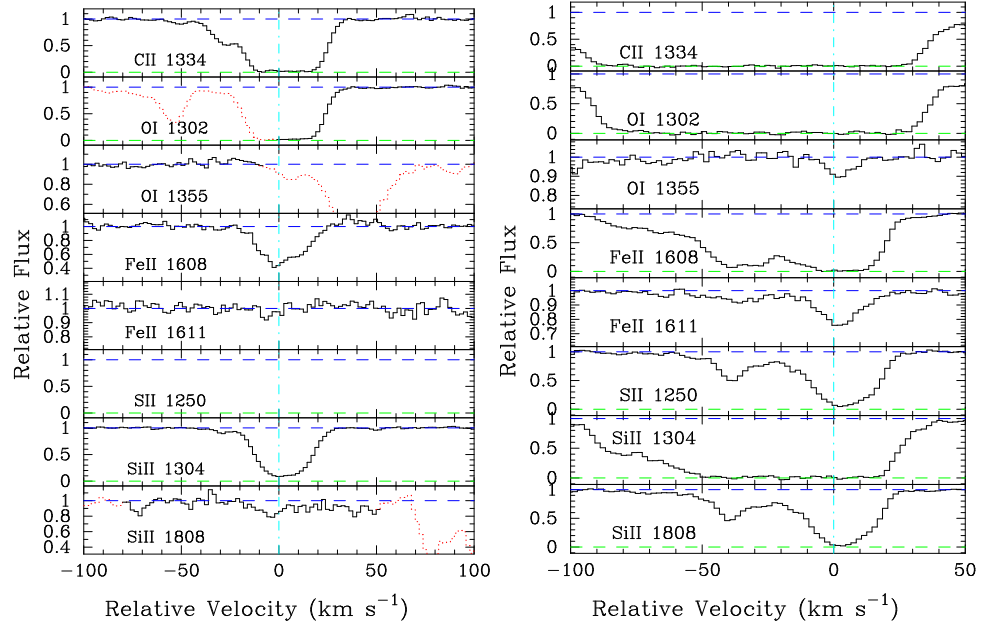


Figure 6: Velocity profiles of metal-line transitions for (a) the metal-poor damped Ly α system at $z = 3.608$ toward Q1108-07 and (b) the metal-strong damped Ly α system at $z = 2.626$ toward Q0812+32. *Grey* indicates the range of flux between 0 and 1. *Red* lines are blends due to other transitions.

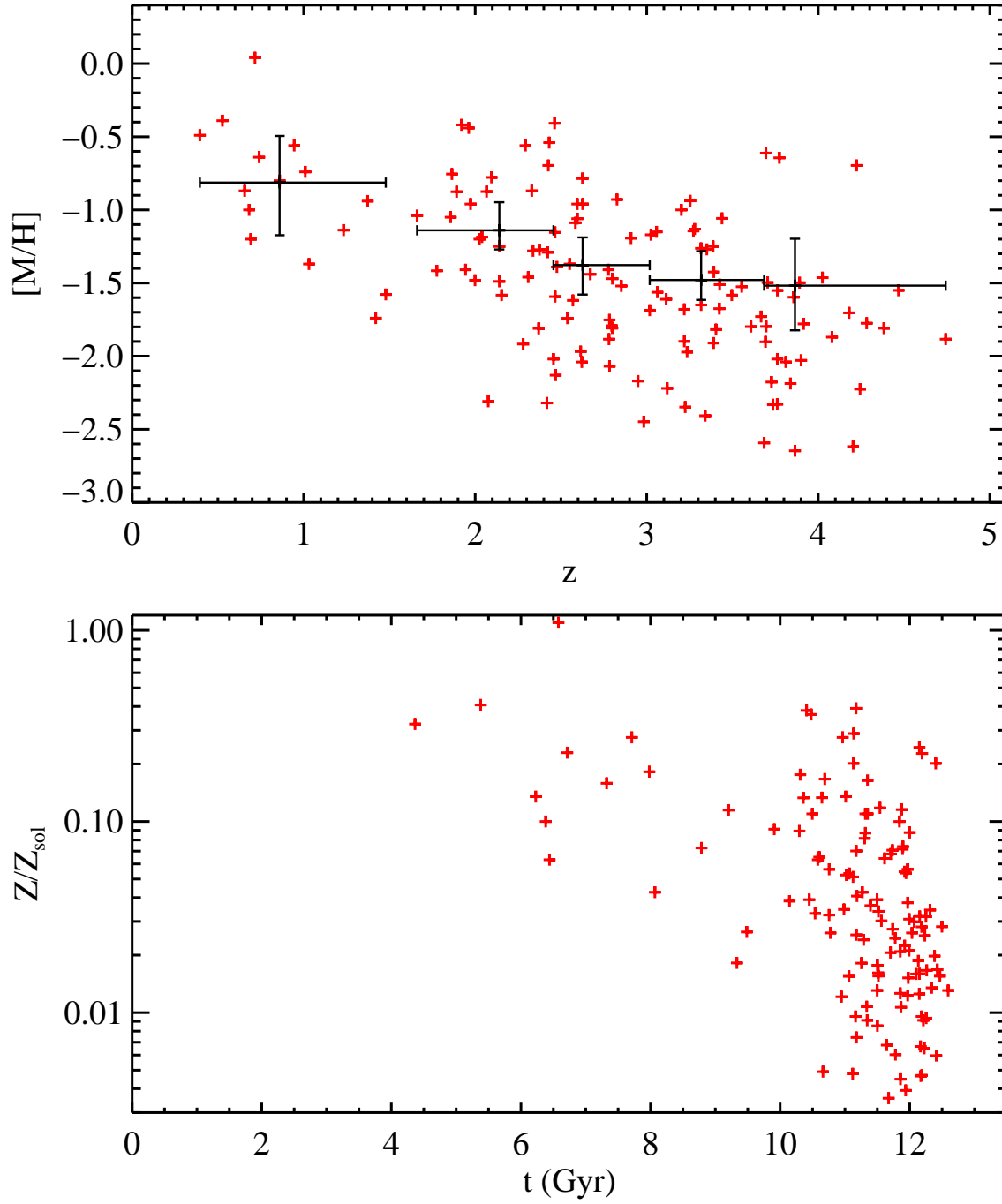


Figure 7: Current summary of the metallicity measurements of the damped Ly α systems as summarized in Prochaska et al. (2003a), Kulkarni et al. (2005), and Rao et al. (2005). The upper panel plots metallicities against redshift and the binned points indicate the cosmological mean metallicity with 95% c.l. uncertainty. The lower panel plots the metallicity versus look-back time. The overwhelming majority of observations are from $t > 10$ Gyr.

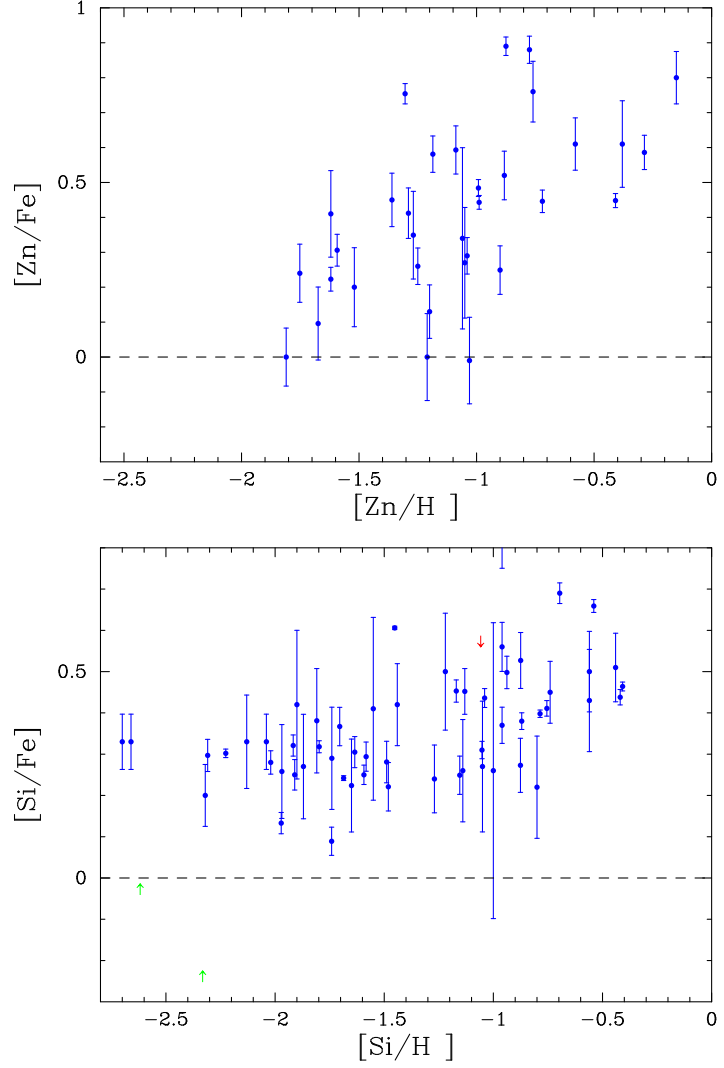


Figure 8: Plot of (a) gas-phase $[\text{Zn}/\text{Fe}]$ observations against Zn metallicity for all damped Ly α systems with high signal-to-noise echelle observations and (b) gas-phase $[\text{Si}/\text{Fe}]$ observations against Si metallicity for all damped Ly α systems with high signal-to-noise echelle observations. Damped Ly α systems with upper limits to Zn were suppressed from panel (a).

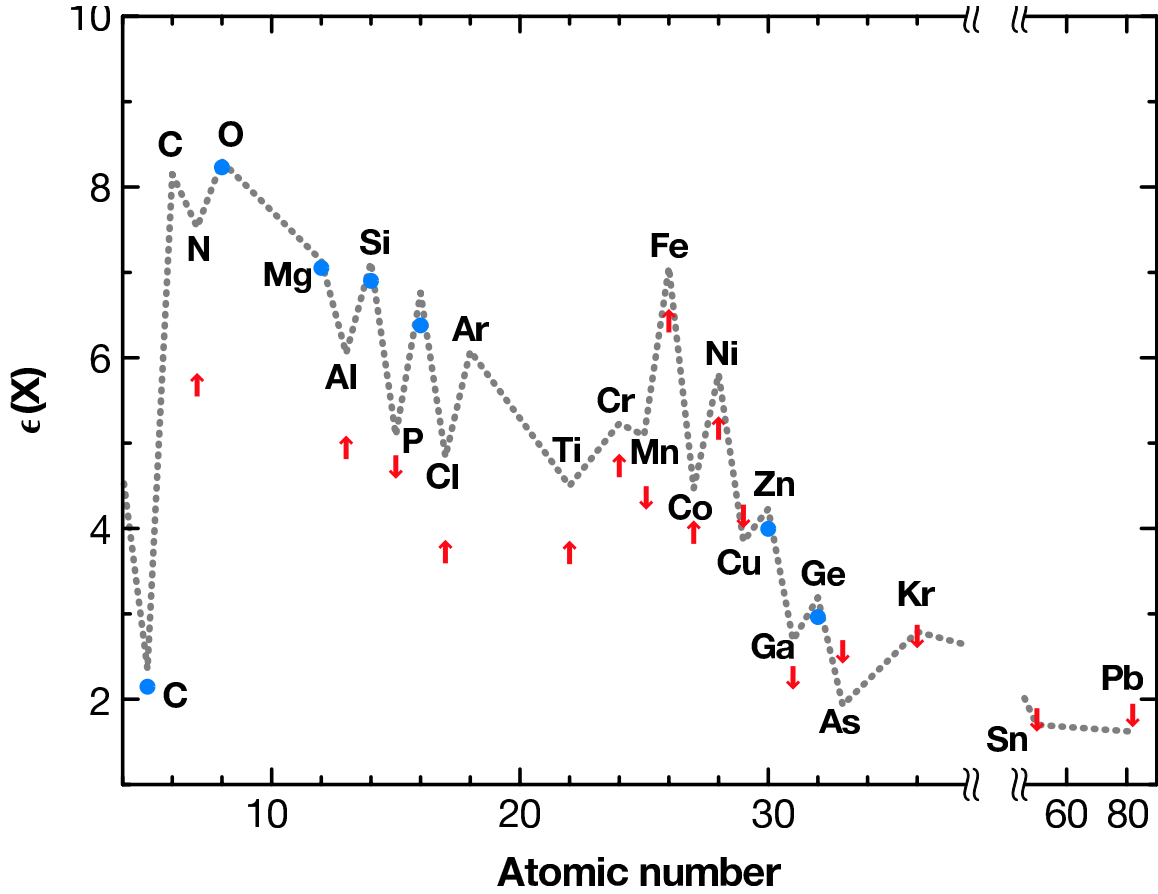


Figure 9: Abundance pattern for the metal-strong damped $\text{Ly}\alpha$ system at $z = 2.626$ toward Q0812+32. Because of the high metal abundance, $[\text{O}/\text{H}] = -0.44$, a dust correction is necessary, and in this case a conservative ‘warm halo’ correction (Savage & Sembach 1996) was applied. The dotted line traces the Solar abundance pattern scaled to match the oxygen abundance of the damped $\text{Ly}\alpha$ system.

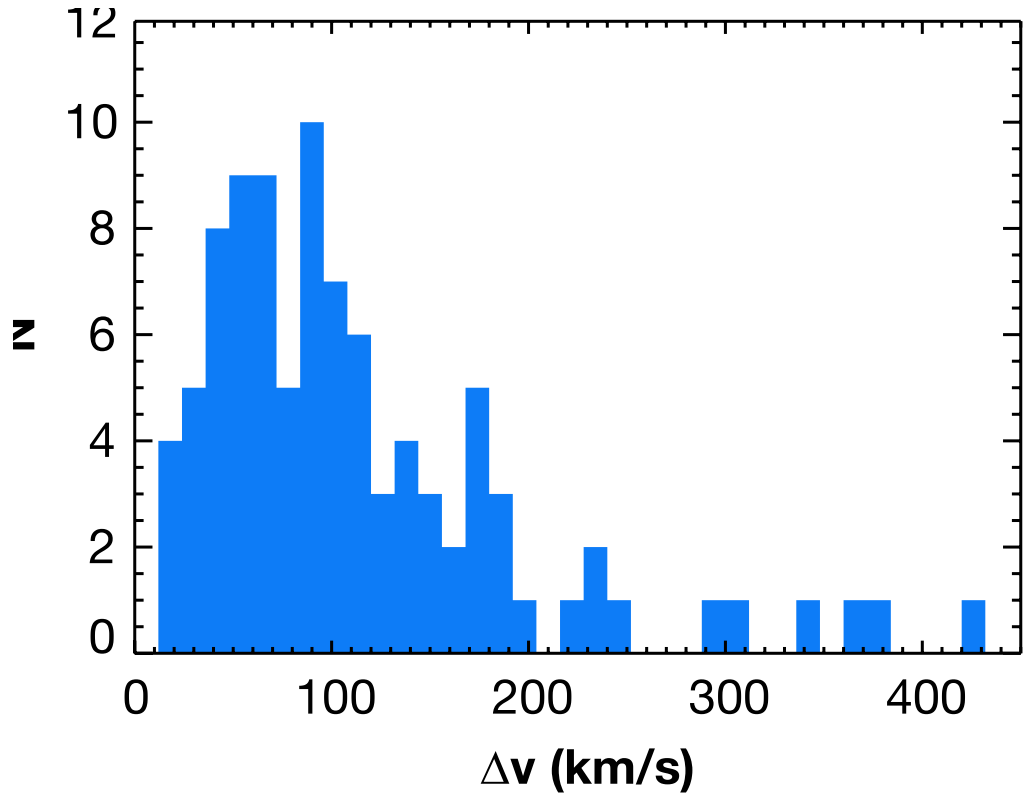


Figure 10: Histogram of the low-ion velocity widths for the current sample of damped Ly α systems with HIRES, UVES, or ESI observations. The median Δv value is 90 km s^{-1} and the distribution shows a significant tail to beyond 200 km s^{-1} .

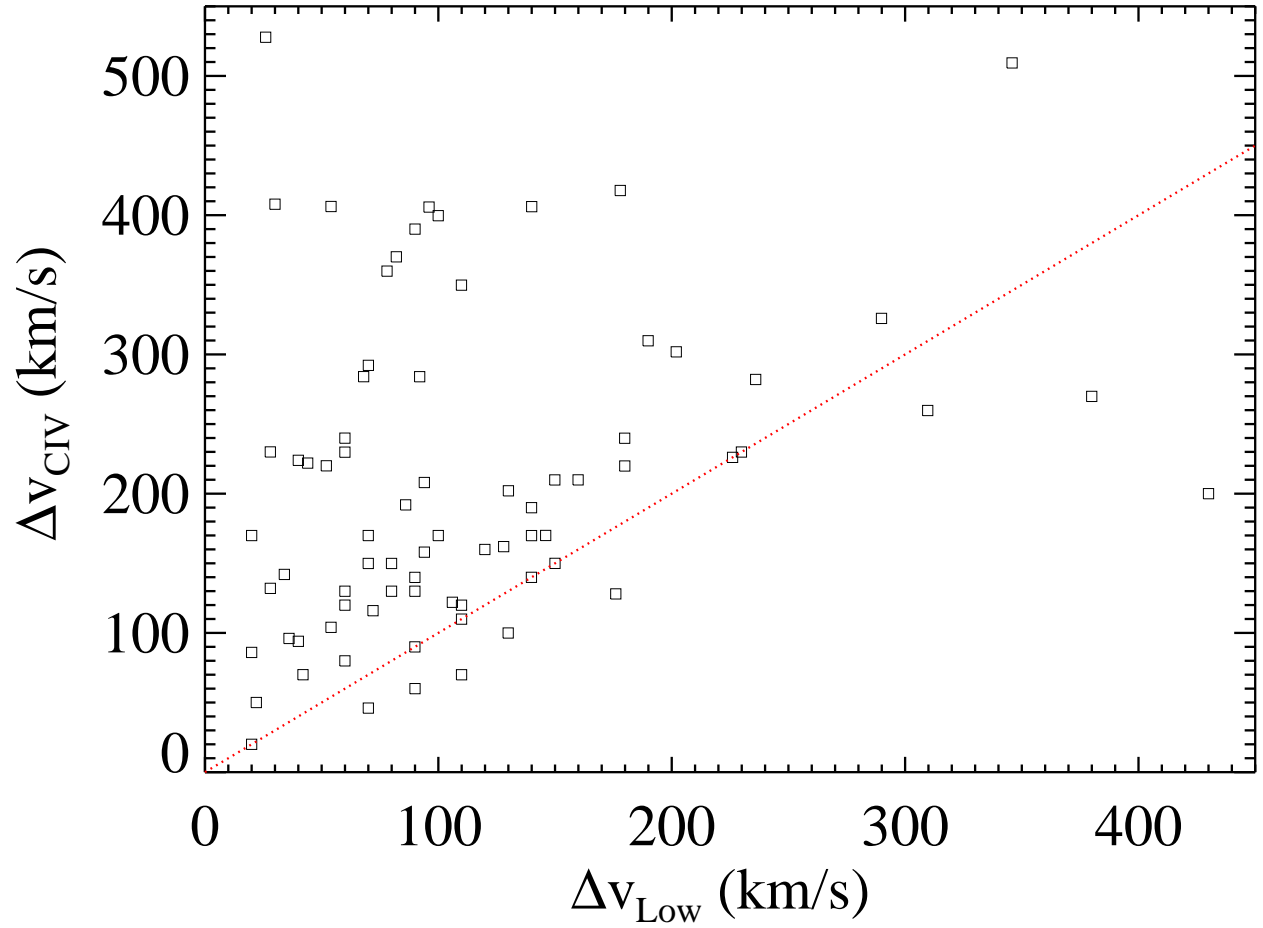


Figure 11: Comparison of the CIV velocity width with the low-ion velocity width for the current sample of damped $\text{Ly}\alpha$ systems with HIRES or ESI observations. With only one or two exceptions, $\Delta v_{\text{CIV}} > \sim \Delta v_{\text{Low}}$.

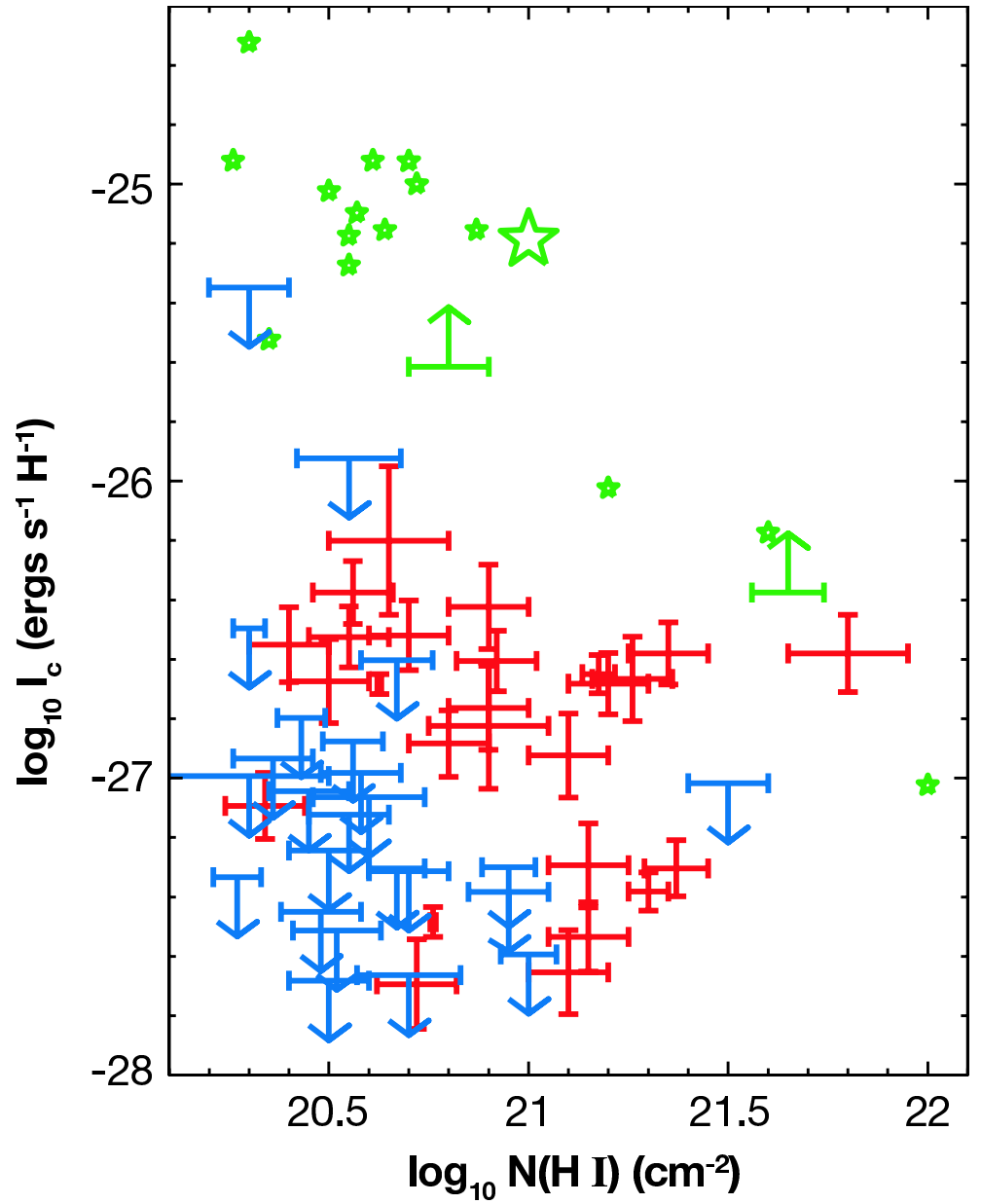


Figure 12: ℓ_c versus $N(\text{H I})$ for sample of 52 damped Ly α systems. *Red* data points are positive detections, *blue* are 2σ upper limits, and *green* are 2σ lower limits. Small stars depict positive detections from sightlines in the Galaxy ISM. Large star depicts [C II] 158 μm emission rate per H atom averaged over the disk of the Galaxy. The latter is about 30 times higher than the average of the DLA detections.